

2023-08-01

## Using Stable Water Isotopes and Radiogenic Strontium Isotopes to Trace Water and its Salinity Sources in Pecos and Colorado River Basins in Texas

Nuria Valeria Andreu Garcia  
*University of Texas at El Paso*

Follow this and additional works at: [https://scholarworks.utep.edu/open\\_etd](https://scholarworks.utep.edu/open_etd)



Part of the [Environmental Sciences Commons](#), and the [Hydrology Commons](#)

---

### Recommended Citation

Andreu Garcia, Nuria Valeria, "Using Stable Water Isotopes and Radiogenic Strontium Isotopes to Trace Water and its Salinity Sources in Pecos and Colorado River Basins in Texas" (2023). *Open Access Theses & Dissertations*. 3893.

[https://scholarworks.utep.edu/open\\_etd/3893](https://scholarworks.utep.edu/open_etd/3893)

This is brought to you for free and open access by ScholarWorks@UTEP. It has been accepted for inclusion in Open Access Theses & Dissertations by an authorized administrator of ScholarWorks@UTEP. For more information, please contact [lweber@utep.edu](mailto:lweber@utep.edu).

USING STABLE WATER ISOTOPES AND RADIOGENIC STRONTIUM ISOTOPES TO  
TRACE WATER AND ITS SALINITY SOURCES IN  
PECOS AND COLORADO RIVER BASINS  
IN TEXAS

NURIA VALERIA ANDREU GARCIA  
Master's Program in Environmental Science

APPROVED:

---

Lin Ma, Ph.D., Chair

---

Alex Mayer, Ph.D., Co-Chair

---

Hernan Moreno, Ph.D.

---

Stephen L. Crites, Jr., Ph.D.  
Dean of the Graduate School

Copyright 2023 Nuria Valeria Andreu Garcia

## **DEDICATION**

To everyone who has been there for me during my happiest and saddest moments. My breakdowns and bursts of joy. This is also for me and a new beginning.

A mis papas, mi franco y seguro puerto. Gracias por ser la parte más sólida de mí, apoyarme y escucharme cuando sentí que no podía más. Les dedico este logro desde el fondo de mi corazón.

A mis hermanos que me ayudaron a ver las cosas diferentes y siempre ver el lado bueno de cada situación. Que me animaron siempre, sé que puedo contar con ustedes en cualquier momento.

To my UTEP friends who made this trajectory one of the best experiences of my life. I wouldn't have done it without all of you. We were going through the same process but always supported each other and put a smile on our faces when frustration/stress was our worst enemy.

To my all-time friends who always knew I could do great things. Thank you for your patience, support, and all-time love.

Finally, thanks to me. My younger self is extremely proud of who I have become and where I am going. I always knew I was making the right decision to follow my love for the environment.

USING STABLE WATER ISOTOPES AND RADIOGENIC STRONTIUM ISOTOPES TO  
TRACE WATER AND ITS SALINITY SOURCES IN  
PECOS AND COLORADO RIVER BASINS  
IN TEXAS

By

NURIA VALERIA ANDREU GARCIA, B.S.

THESIS

Presented to the Faculty of the Graduate School of  
The University of Texas at El Paso  
in Partial Fulfillment  
of the Requirements  
for the Degree of

MASTER OF SCIENCE

Department of Earth, Environmental, and Resource Sciences

THE UNIVERSITY OF TEXAS AT EL PASO

August 2023

## **ACKNOWLEDGMENTS**

I want to thank the Department of Earth, Environmental, and Resource Sciences for being a second home over the last seven years. Specially Dr. Lin Ma for being my mentor and an amazing guide for the last two years. Having him as an advisor has been the best and most valuable experience. I also want to thank graduate students in Dr. Hugo Gutierrez's lab for explaining and mentoring me. Lastly, I want to thank my lab friends whom I mentored and who always were open to helping and learning new things.

Lastly, I want to thank Dr. Alex Mayer and Dr. Hernan Moreno for being part of my committee and guiding me through this journey.

## ABSTRACT

Water stable isotope ratios (Deuterium/hydrogen  $^2\text{H}/^1\text{H}$  and Oxygen  $^{18}\text{O}/^{16}\text{O}$  ratios) and radiogenic strontium isotope ratios ( $^{87}\text{Sr}/^{86}\text{Sr}$ ) have been widely used to trace various hydrologic processes and understand surface-groundwater interactions for watershed and critical zone studies. Our project aimed to trace the water and salinity sources in the Colorado and Pecos Rivers, two major rivers that provide essential water resources for water-stressed parts of Texas. In our study, we collected water samples from 25 locations during July (monsoon season), December 2021 (dry season), and May 2022 (pre-monsoon season) along the Pecos and Colorado rivers from central Texas to the Gulf of Mexico. Our project used water-stable isotope ratios to understand water source/age, evaporation, groundwater recharge, and discharge as stable isotope water signatures reflect water source regions' altitude, latitude, and seasonality. Our project also used strontium isotope ratios to trace the salinity sources from water-rock interactions in watersheds. In addition, a trace metals study was included to understand human and industrial presence on both rivers.

Water stable isotope ratios were analyzed to identify the water source from each location using Picarro L2130-*i* Isotope and Gas Concentration Analyzer and then compared to the global meteoric water line (GWML). Sr isotope ratios were analyzed using Nu Plasma Multi-collector inductively coupled plasma mass spectrometer (MC-ICPMS). Trace metals were completed using a Thermo Fisher Scientific iCAP RQ ICP-MS. Field measurements were conducted at each location, including DO, conductivity, TDS, pH, ORP, and temperature, with a YSI ProQuatro Multiparameter Meter and a field alkalinity test. Geology and land use information were obtained from multiple public sources and analyzed by independent research teams on this project. Water stable isotope results indicate highly saline brine upwelling in the upper reaches of the Pecos and Colorado Rivers. The middle portion shows the absence of brine contributions from a carbonate

aquifer, resulting in water dilution. The lower portion of the Colorado has more precipitation and brine signatures in drier seasons. Upwelling brines in the upper Pecos and Colorado rivers also contribute to higher  $^{87}\text{Sr}/^{86}\text{Sr}$  ratios and Arsenic concentrations, with both elements associated with shallow and deep brines in the region. Brines may flow through the middle stream in the main river channel and ultimately reach the lower portion of the river during periods of low to no rainfall. Our study highlights that water stable isotope ratios and strontium isotope ratios provide simple yet significant background information for scientific research and water management strategies, such as understanding primary river water sources, salinity sources, mixing with other sources, as well as how rapidly water is moving and where it is stored in the watershed.



## TABLE OF CONTENTS

ACKNOWLEDGMENTS .....	v
ABSTRACT .....	vi
TABLE OF CONTENTS.....	viii
LIST OF TABLES .....	x
LIST OF FIGURES .....	xi
CHAPTER 1: INTRODUCTION .....	1
1.1 MOTIVATION .....	1
1.2 BACKGROUND .....	3
<i>Definition of a watershed bottom and flow paths</i> .....	3
<i>Water stable isotope ratios</i> .....	5
<i>Seasonal <math>\delta^{18}\text{O}</math> trends in rainwater</i> .....	8
<i>Spatial and elevation <math>\delta^{18}\text{O}</math> trends in rainwater</i> .....	8
<i>Human impacts on <math>\delta^{18}\text{O}</math> trends in rainwater</i> .....	8
<i><math>^{87}\text{Sr}/^{86}\text{Sr}</math> Isotope ratios</i> .....	9
1.3 OBJECTIVES .....	12
CHAPTER 2: METHODOLOGY .....	13
2.1 SITE DESCRIPTION .....	13
<i>Pecos River and groundwater aquifers</i> .....	13
<i>Colorado River and groundwater aquifers</i> .....	15
2.2 SAMPLE COLLECTION AND FIELD ANALYSIS .....	18
2.3 SAMPLING – RELATED LIMITATIONS .....	20
2.4 LABORATORY ANALYSIS .....	21
2.5 WATER STABLE ISOTOPES RATIO ANALYSIS.....	21
2.6 QUALITY ASSURANCE QUALITY CONTROL ON STABLE ISOTOPE RATIO ANALYSIS.....	26
<i><math>^{87}\text{Sr}/^{86}\text{Sr}</math> Isotope Analysis</i> .....	26
CHAPTER 3: RESULTS .....	28
3.1 WATER STABLE ISOTOPES: $\delta^{18}\text{O}$ and $\delta\text{D}$ ratios.....	28
3.2. <i>Electrical conductivity values</i> .....	30

3.3. $^{87}\text{Sr}/^{86}\text{Sr}$ ISOTOPES RATIOS AND CORRELATION WITH $\delta^{18}\text{O}$ RATIOS.....	33
3.4. HEAVY METALS.....	40
3.4.1 <i>Pecos River</i> .....	40
3.4.2 <i>Colorado River</i> .....	45
3.4.4 T-Test.....	50
3.4.5 IMPLICATIONS FOR SOCIETY AND ECOSYSTEMS .....	52
CHAPTER 4: DISCUSSION.....	53
4.1 WATER STABLE ISOTOPES: WHERE IS THE WATER COMING FROM DIFFERENT PORTIONS OF THE WATERSHED? .....	53
4.2 STRONTIUM ISOTOPES RATIO .....	59
4.3 TRACE METALS .....	61
CHAPTER 5: CONCLUSION .....	64
REFERENCES .....	66
VITA.....	69

## LIST OF TABLES

Table 1. Reference values from Picarro Chemcorrect. ....	26
Table 2. Student's T-test paired two samples of means. ....	51

## LIST OF FIGURES

Figure 1. River Basins and Rainfall Map of Texas (BEG Maps of Texas).....	2
Figure 2. Geology of Texas (TX Almanac, n.d.).....	2
Figure 3. Texas population map (Wikimedia commons, n.d.).....	3
Figure 4. Conceptual model of watershed boundaries modified from Condon et al., 2020. ....	4
Figure 5. Diagram illustrating the impact of human activity on the $\delta D$ and $\delta^{18}O$ values of river water in urban areas from Li et al. ....	6
Figure 6. The meteoric relationship for $^{18}O$ and $^2H$ was used to compare stable isotope ratios in our water samples. The figure was modified from Environmental Isotopes in Hydrogeology p.37 (Clark & Fritz, 1997). ....	7
Figure 7. Modified diagram from Bataille et al, illustrating $^{87}Sr/^{86}Sr$ variations in major bedrock lithologies in the USA. Major bedrock model (A). Average $^{86}Sr/^{86}Sr$ values in the United States (B).....	10
Figure 8: Pecos River drainage system (Yuan & Miyamoto, 2008).....	15
Figure 9: Pecos River watershed with locator map of Texas.....	15
Figure 10. DEM of Colorado River Watershed.....	16
Figure 11. Major aquifers map. (Texas Development Board, n.d.).....	18
Figure 12. Pecos and Colorado rivers and basins with numbered sampling locations (Ward, n.d.). .....	19
Figure 13. Cryogenic vacuum extraction setup. A) Edwards Vacuum Pump, B) Fisherbrand Isotemp Digital Block Heaters, C) Thermos Stainless steel container, D) PolyScience immersion probe cooler, E) Glass vials. ....	23
Figure 14. Cryogenic river water extraction: Glass test tubes with frozen samples at $-50^{\circ}C$ in a Thermos stainless steel container. In addition to evaporating samples in Fisherbrand Isotemp Digital Block Heaters.....	24
Figure 15. Cavity Ringdown Spectrometer Picarro L2130-i Isotope and Gas Concentration Analyzer.....	25
Figure 16. Laboratory analysis for Sr isotopes. Plastic columns with strontium resin and sample. .....	27
Figure 17. $\delta^2H$ and $\delta^{18}O$ (‰VSMOW) plot all eight sample sites from July 2021 to December 2021. The Global Meteoric Water Line (GMWL) is a standard value $\delta^2H= 8 * \delta^{18}O + 10‰$ SMOW. ....	29
Figure 18. $\delta^2H$ and $\delta^{18}O$ (‰VSMOW) plot of all seventeen sample sites from July 2021, December 2021, and May 2022. The Global Meteoric Water Line (GMWL) is a standard value $\delta^2H= 8 * \delta^{18}O + 10‰$ SMOW.....	30
Figure 19. $\delta^{18}O$ and Electrical Conductivity (EC) plot of all eight sample sites from July 2021 and December 2021. EC concentration is higher with samples 3, 9, and 10.....	31
Figure 20. $\delta^{18}O$ and Electrical Conductivity (EC) plot of all seventeen sample sites from July 2021, December 2021, and May 2022. ....	32
Figure 21. $^{87}Sr/^{86}Sr$ and $\delta^{18}O$ isotopic ratio plot of all eight sample sites from July 2021 and December 2021.....	33
Figure 22. $^{87}Sr/^{86}Sr$ and $\delta^{18}O$ isotopic ratio plot of all seventeen sample sites from July 2021, December 2021, and May 2022.....	35
Figure 23. $^{87}Sr/^{86}Sr$ and $1/Electrical\ Conductivity$ plot of all eight sample sites from July 2021 and December 2021. ....	36

Figure 24.  $^{87}\text{Sr}/^{86}\text{Sr}$  and  $1/\text{Electrical Conductivity}$  plot of all seventeen sample sites from July 2021, December 2021, and May 2022. .... 37

Figure 25.  $^{87}\text{Sr}/^{86}\text{Sr}$  ratio vs  $1/^{88}\text{Sr}$  illustrating mixing trends among multiple data points. The relationship between these isotopic ratios provides insights into the mixing processes within the studied system. Points on  $1/^{88}\text{Sr}$  closer to 0 represent a high concentration. .... 38

Figure 26.  $^{87}\text{Sr}/^{86}\text{Sr}$  ratio vs  $1/^{88}\text{Sr}$  illustrating mixing trends among multiple data points. The relationship between these isotopic ratios provides insights into the mixing processes within the studied system. Points on  $1/^{88}\text{Sr}$  closer to 0 represent a high concentration. .... 39

Figure 27. Arsenic (As) values in parts per billion (ppb) of the Pecos River..... 40

Figure 28. Lead (Pb) values in parts per billion (ppb) of the Pecos River. .... 41

Figure 29. Boron (B) values in parts per billion (ppb) of the Pecos River. .... 42

Figure 30. Cadmium (Cd) values in parts per billion (ppb) of the Pecos River. .... 43

Figure 31. Vanadium (V) values in parts per billion (ppb) of the Pecos River. .... 44

Figure 32. Colorado River Arsenic (As) values in parts per billion. .... 46

Figure 33. Colorado River Lead (Pb) values in parts per billion..... 47

Figure 34. Colorado River Boron (B) values in parts per billion. .... 48

Figure 35. Colorado River Cadmium (Cd) values in parts per billion..... 49

Figure 36. Colorado River Vanadium (V) values in parts per billion. .... 50

Figure 37.  $\delta^2\text{H}$  and  $\delta^{18}\text{O}$  (‰VSMOW) plots portraying the distribution of all samples divided into three sections: upper, middle, and lower. The upper portion of the Colorado River with samples 1 to 6 (A). The upper portion of the Pecos River with samples 3, 9, and 10 (B). The middle portion of the Colorado River with samples 7 to 11 (C). The middle portion of the Pecos River with samples 11 to 15.5 (D). The lower portion of the Colorado River with samples 12 to 15 (E). The Global Meteoric Water Line (GMWL) is a standard value  $\delta^2\text{H} = 8 * \delta^{18}\text{O} + 10$ ‰ SMOW. .... 57

Figure 38. The sedimentary brines conceptual model of groundwater mixing was modified from Dutton et al., 1989..... 58

# CHAPTER 1: INTRODUCTION

## 1.1 MOTIVATION

This project aims at investigating the influence of climate, lithology, and human activities on water and salinity sources in major watersheds in Texas, using water and salinity tracers including stable water isotopes (oxygen and hydrogen:  $\delta^{18}\text{O}$  and  $\delta\text{D}$ ), strontium isotope ratios ( $^{87}\text{Sr}/^{86}\text{Sr}$ ), as well as trace elemental concentrations. To achieve this, two major Texas river basins, Pecos and Colorado rivers, were selected as study areas based on four specific factors: (1) the mean annual precipitation values decrease systematically from east to west across these two watersheds (Figure 1); (2) the subsurface geology in these two watersheds characterized by systematic changes of lithologies (limestone, sandstone, mudstone, and evaporite; Figure 2); (3) the uneven distribution of human population in Texas across these two watersheds, with a higher population and more urban centers on the eastern side and developed land used for farming and agriculture in the rest of the state (Figure 3); and (4) the constant physical erosion conditions, tectonic dormancy, and low-relief landscapes that create an ideal research setting for investigating the changes of climate, lithology, and human impacts across the two watersheds.

The stable oxygen and hydrogen isotope ratios of water can be used to trace water sources and their pathways in watersheds, understand the interactions between groundwater and surface water, and evaluate the impact of human activities, such as oil and natural gas development, urban and agricultural water uses, on water quality and resource management. The strontium isotope ratios in river water can be used to trace the salinity source resulted from water-rock interactions with dominant lithology types such as with changes from evaporites, carbonates to silicate minerals from upstream to downstream in both watersheds. Finally, the combination of stable water isotope and strontium isotope ratios with trace element concentrations provides insights to investigate the

human impacts on water quality in these two watersheds. The study focuses on investigating the seasonality patterns of these two watersheds by study the river chemistry changes during an entire year, spanning from the monsoon season (June to September 2022) to the dry season (October. 2022 to May 2023). In the region under investigation, the monsoon season is a significant source of surface water, which plays a vital role in providing a steady water supply for rivers and groundwater recharge throughout the state. River basins in Texas are highly important for both society since they are the main water source for the whole state. Both surface and groundwater play a vital role in sustaining the entire state society's and industry's daily needs. Society-wise, multiple cities/communities rely on the river's water supply in addition to agriculture, irrigation, and daily activities. Water is an essential economic and health factor every citizen should be allowed to use. Water resources management is essential in its administration and utilization for every need. It is also important to mention the economic factor water plays daily.



**Figure 1.** River Basins and Rainfall Map of Texas (BEG Maps of Texas).



**Figure 2.** Geology of Texas (TX Almanac, n.d.)

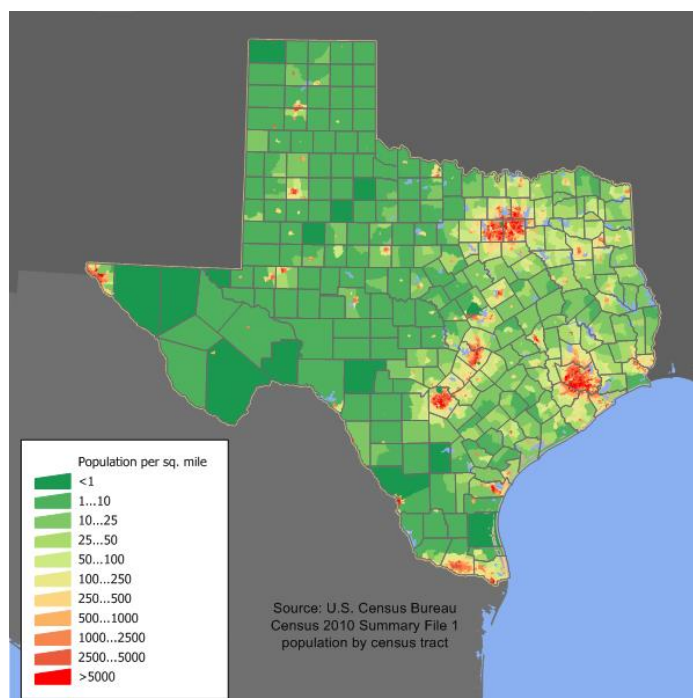


**Figure 3.** Texas population map (“File:Texas population map.png - Wikimedia Commons,” n.d.)

Our investigation includes field sampling for water chemistry, laboratory analyses for isotope ratios, and site characterization on rock lithology, precipitation, and land use. Preliminary investigations were conducted utilizing previous studies of historical river chemistry, GIS analysis, and flow data to select the best river sampling locations. In addition, online datasets from the U.S. Geological Survey (USGS) and Texas Water Development Board (TWDB) were used to obtain historical river chemistry and flow monitoring data.

## 1.2 BACKGROUND

### *Definition of a watershed bottom and flow paths*

The definition of the bottom of a watershed is subject to various types of research fields and focuses, and the extent of the deepest level of a watershed is often not well-defined (Condon et al., 2020). Condon et al. (2020) offered useful insights into accurately describing the bottom of a watershed with respect to different spatial scales, water residence time, and watershed properties



(Figure 4). It is generally known that local to regional groundwater naturally recharges from topography high areas and that groundwater discharge at topography low areas comprises both shallow and deep flow paths with various water residence time. It is imperative to acknowledge that determining “the bottom of the watershed” may vary based on time scales, location, and research objectives. For example, watershed and land surface models (LSM) focused on depth penetrating the soil approximately 2-3 meters while modern groundwater can be found at depths reaching 250 meters (Condon et al., 2020). Critical zone studies have investigated multiple tens of meters more profound into the subsurface than integrated groundwater-surface models, which only examine upper 10 m of depth (Condon et al., 2020). In this project, we follow the critical zone definition of the bottom of the watershed and focus on upper 100 m level of the watershed that has modern groundwater and relatively short residence time. We assume this type of water represents the dominant water source that discharges from groundwater into surface water such streams and rivers in a watershed.

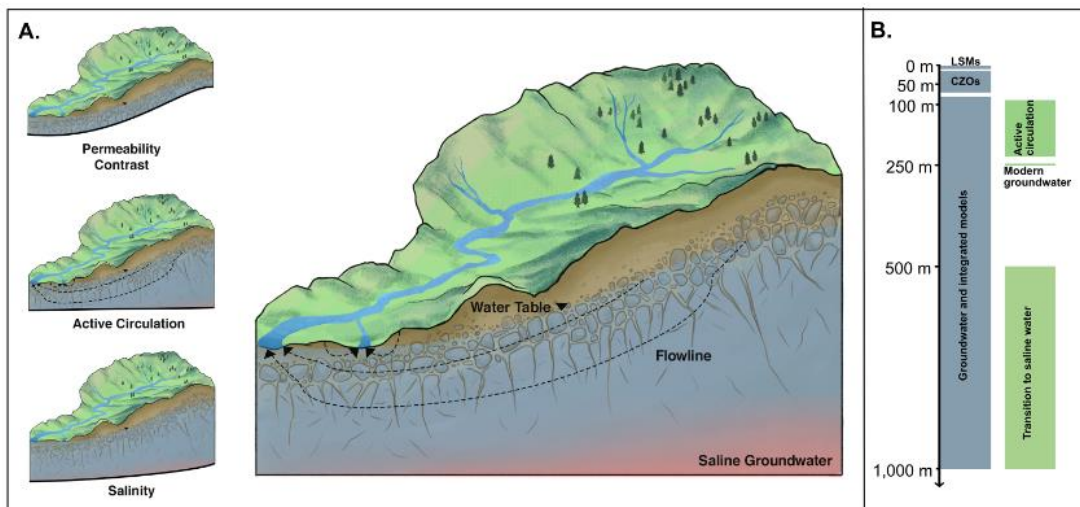


**Figure 4.** Conceptual model of watershed boundaries modified from Condon et al., 2020.

### ***Water stable isotope ratios***

Water stable isotope ratios of oxygen and hydrogen (defined as  $\delta^{18}\text{O}$  and  $\delta\text{D}$  ratios) have been widely utilized in watershed and critical zone studies to understand various hydrologic processes and surface-groundwater interactions. They can also be used to trace water-rock interactions, groundwater recharge, and other subsurface hydrologic processes, making them a valuable tool in tracing water pathways, solutes, and contaminants in hydrogeology (Clark & Fritz, 1997). Generally, water molecules consist of two isotopes of hydrogen, H with one proton, D (deuterium) with one proton and one neutron, and two common stable oxygen isotopes,  $^{18}\text{O}$  (8 protons and 10 neutrons) and  $^{16}\text{O}$  (8 protons and 8 neutrons). The O and H isotope ratios in these water molecules depend on a mass dependent isotope fractionation process (Souchez et al., 2002). The initial stage in establishing the isotopic correlation between the  $\delta^{18}\text{O}$  and  $^2\text{H}$  composition of meteoric waters is from the process of oceanic evaporation (Clark & Fritz, 1997). The subsequent isotopic correlation between  $\delta^{18}\text{O}$  and  $^2\text{H}$  in meteoric waters arises from fractionation during the condensation stage from water vapor mass during rainout events. For example, during rain formation and precipitation, the rain is enriched in  $^{18}\text{O}$  and D relative to  $^{16}\text{O}$  and H, respectively, and the residual vapor becomes depleted in  $^{18}\text{O}$  and D due to fractionation. As a result, heavier isotopes are lost relative to lighter isotopes during rainout events, which enhances the lighter isotopes in the remaining water vapor or clouds. (Clark & Fritz, 1997). Indeed, the classic Rayleigh distillation during rainout is the main factor that induces changes in water stable isotope ratios in rainwater from different seasons and locations across Earth's surface (Figure 5). Hence, warmer regions typically exhibit enriched and heavier waters with higher values, while colder regions are associated with depleted waters and low values as the rain moves from tropical oceans toward cold polar regions (Clark & Fritz, 1997).

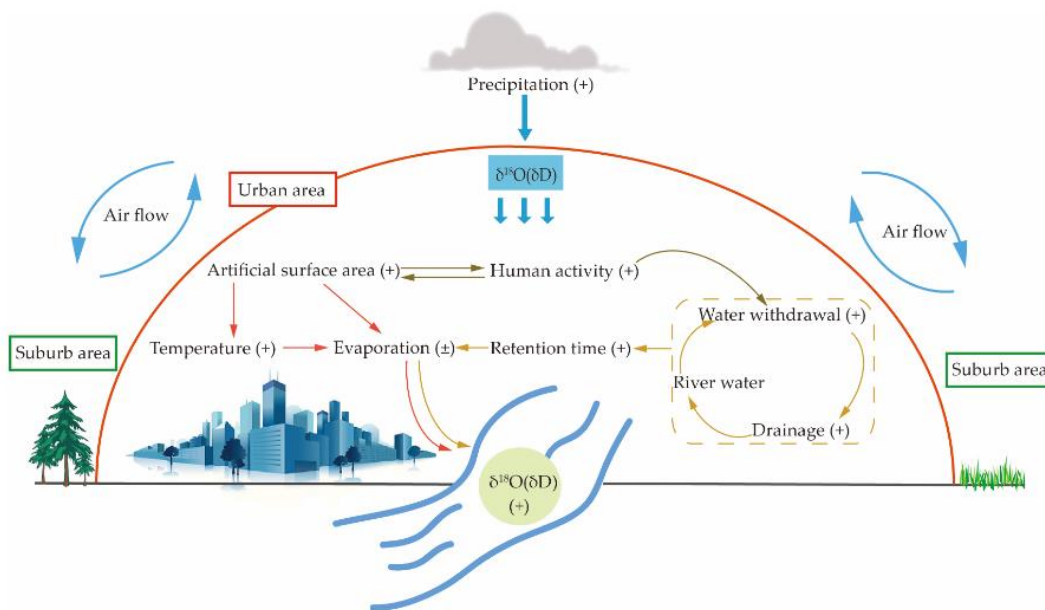


**Figure 5.** Diagram illustrating the impact of human activity on the  $\delta D$  and  $\delta^{18}O$  values of river water in urban areas from Li et al (Li et al., 2019).

On a global scale, the well-established Craig's global meteoric water line (GMWL) represents a simple relationship between  $^{18}O$  and  $^2H$  in fresh surface waters as  $\delta^2H = 8 \delta^{18}O + 10\text{‰}$  (SMOW). This general pattern characterizes the global trend of surface water samples (rain, streams, rivers, local and regional groundwater) with diverse climatic and geographic factors (Figure 6). Rainwater recharge typically results in the formation of shallow groundwater near the GMWL, while an evaporation trend will result a shallower slope on the  $^{18}O$  and  $^2H$  relationship and its deviation from the GMWL. Hence, water with evaporation occurring from surface water reservoirs is characterized by signature values falling below the GMWL, distinct from other water endmembers. In Figure 6, O and H isotope ratios of selected Texas rain samples, shallow groundwater, deep basin brines were compared to Craig's GMWL. The different stable isotope

signatures in these proposed water endmembers will help to understand surface-groundwater interactions and water quality in Texas rivers.

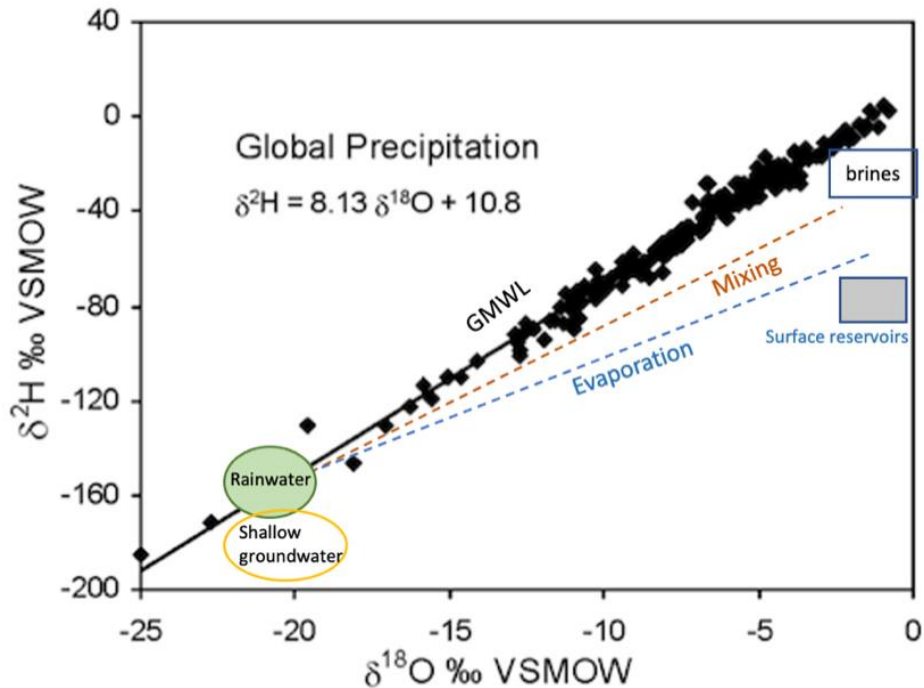


**Figure 6.** The meteoric relationship for  $^{18}\text{O}$  and  $^2\text{H}$  was used to compare stable isotope ratios in our water samples. The figure was modified from Environmental Isotopes in Hydrogeology p.37 (Clark & Fritz, 1997).

Determining the local meteoric water line (LMWL) involves averaging multiple data points of precipitation, accounting for factors such as rainfall evaporation, seasonality, and water vapor mass (Clark & Fritz, 1997). In regional or local studies, the incorporation of an LMWL is crucial. However, continuous precipitation monitoring over a specific timeframe may only sometimes be practicable. Therefore, our study adopted the LMWL obtained from literatures whose stations are close to our study area. In the results section, a description of each stable isotope plot will be provided, along with an accompanying explanation of the corresponding local meteoric water line.

### ***Seasonal $\delta^{18}\text{O}$ trends in rainwater***

The stable isotope values of water can exhibit seasonal variability, which a range of environmental factors, such as precipitation and temperature, can influence. Based on the global map of  $^{18}\text{O}$ , it has been determined that the range of  $^{18}\text{O}$  found in rainfall in Texas falls between -8 and -6 (Clark & Fritz, 1997). It is essential to mention that stable isotope values in rain increase toward the tropical regions, on the contrary, decrease in colder areas.

### ***Spatial and elevation $\delta^{18}\text{O}$ trends in rainwater***

The stable isotope ratios of precipitation exhibit lower values at higher altitudes, typically ranging from 2 to 3‰ lower when compared to low altitude precipitations. When analyzing groundwater oxygen isotope values, lower stable isotope ratios may indicate higher elevations if the altitude of the ground surface elevation is the primary factor controlling these values (Uliana et al., 2007). Similarly, Dansgaard's analysis of  $\delta^{18}\text{O}$  and temperature relationship plot indicates that precipitation at higher latitudes typically exhibits more negative  $\delta^{18}\text{O}$  values (Clark & Fritz, 1997). Specifically, continental stations in North America demonstrate a variation of about 0.6‰ for each degree of latitude in  $\delta^{18}\text{O}$  values (Clark & Fritz, 1997). Our sample's latitudes range from 28°18' to 32°37', a four-degree change and suggest the control of latitude on water stable isotope ratios. Given the relatively low elevation change across the state, altitude is not a significant factor influencing the stable isotope ratios of water samples in Texas. In addition, temperature exhibits variation across different seasons and in the west-east direction. As noted by Uliana et al. (2007), cooler precipitation temperatures are primarily associated with lower  $\delta^{18}\text{O}$  values in precipitation.

### ***Human impacts on $\delta^{18}\text{O}$ trends in rainwater***

As previously mentioned, Figure 3 provides information about the distribution of the population across the state of Texas. The population is one of the reasons this state is essential for

our study. Human activities, such as agriculture and other water uses impacted by population growth, can also affect water stable isotopes. Figure 5, based on research by Li et al. (2019), demonstrates the impact of human activities on the  $\delta D$  and  $\delta^{18}O$  of river water in urban areas. The study highlights climate and human activity as the two main factors responsible for this impact. The urban heat island effect, which increases the evaporation fractionation of isotopes, can alter the stable isotope signature of water in urban areas, as illustrated in the diagram (Li et al., 2019). Rainwater infiltrates the ground and may flow through the unsaturated and saturated zones to reach the groundwater aquifer, which then discharges into the river. In addition, human settlements, urban areas, and industrial activities such as oil field companies can contaminate water sources. This contamination process can also alter the water's stable isotope signals of  $\delta D$  and  $\delta^{18}O$ . Therefore, it is essential to consider the potential impact of human activities on the stable isotope composition of water when conducting hydrological studies.

Overall, water stable isotope ratios ( $\delta D$  and  $\delta^{18}O$ ) are a powerful tool in understanding hydrologic processes, geochemical reactions, and groundwater contamination, making them an essential component of many watersheds and critical zone studies.

### ***<sup>87</sup>Sr/<sup>86</sup>Sr Isotope ratios***

Radiogenic  $^{87}\text{Sr}/^{86}\text{Sr}$  isotope ratios are essential in earth science and environmental studies, forensics, and archaeology research (Barbieri et al., 2005); (Crowley et al., 2017). Strontium, a naturally occurring element, has been present in rock formations and in various rock types, such as granites, carbonates, and evaporite rocks, commonly found in our research sites in Texas. Strontium has four stable isotopes, namely  $^{88}\text{Sr}$ ,  $^{86}\text{Sr}$ ,  $^{84}\text{Sr}$ , and  $^{87}\text{Sr}$ , and  $^{87}\text{Sr}$  is produced by the decay of rubidium ( $^{87}\text{Rb}$ ) (Crowley, 2017).  $^{87}\text{Sr}/^{86}\text{Sr}$  isotope ratios in rocks show significant mineral-specific variations, particularly in older rock formations characterized by high Rb/Sr

ratios, and likely exhibit significant high  $^{87}\text{Sr}/^{86}\text{Sr}$  ratios than their younger counterparts (Shand et al., 2009). These can be used for tracing groundwater flow paths. Isotopic fractionation refers to the separation of strontium isotopes during physical or chemical processes, leading to a discernible difference in isotopic composition between the original and processed materials. Such fractionation can occur during precipitation or mineral dissolution, possibly affecting strontium isotopic ratios (Uliana et al., 2007). However, the  $^{87}\text{Sr}/^{86}\text{Sr}$  ratios observed in groundwater in aquifers containing strontium-bearing minerals are anticipated to mirror the isotopic ratio exhibited by such minerals (Uliana et al., 2007). The measured values of these ratios can be utilized to trace regional groundwater flow patterns and to determine any mixing relationships (Uliana et al., 2007).

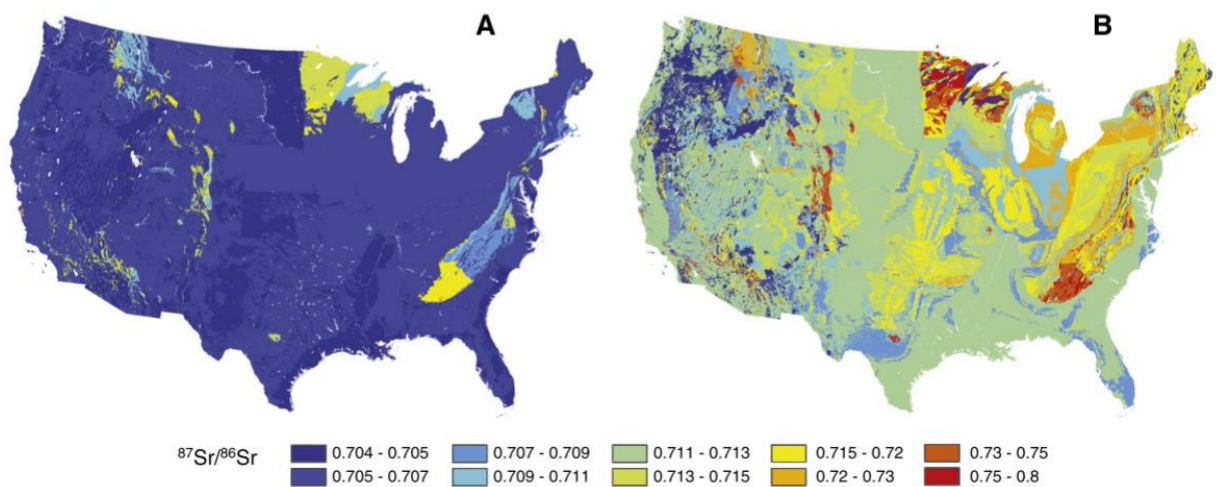


**Figure 7.** Modified diagram from Bataille et al, illustrating  $^{87}\text{Sr}/^{86}\text{Sr}$  variations in major bedrock lithologies in the USA. Major bedrock model (A). Average  $^{86}\text{Sr}/^{86}\text{Sr}$  values in the United States (B).

Depending on different lithologies, our  $^{87}\text{Sr}/^{86}\text{Sr}$  samples expect to have a similar value range as in Figure 7. It displays multiple variations on primary rock lithologies in the USA. Most Sr values fall between 0.704 to 0.816 (Bataille & Bowen, 2012). Depending on different lithologies, we may observe a range of 0.707 to 0.720 for Sr isotope ratio in our samples for most of the Pecos and

Colorado watersheds. In addition, some values in 0.750 to 0.816 for the Llano Uplift area in the Colorado River because of the old and silicate nature of the Llano uplift lithology. By looking into multiple current strontium values and the geology of the sites, we can understand the past hydrological process, duration of precipitation and recharge events, and river trajectory. In addition, the changes in lithology from evaporites and carbonates to silicates can be paired with the strontium values and understand the water-rock interaction through time and with deep basin formations. In the context of our research project, we aimed to investigate water-rock interaction and salinity sources from various dominant lithology types in river basins by tracing and measuring  $^{87}\text{Sr}/^{86}\text{Sr}$  isotopes from our water sample locations, spanning from the start to the coast of the Pecos and Colorado rivers. By analyzing the  $^{87}\text{Sr}/^{86}\text{Sr}$  isotopic composition, we could gain insight into the origin of the dissolved strontium in the water and the dominant lithology types contributing to the salinity of the river systems (Barbieri, 2005).

Brine salinity is another important factor in our research study. Strontium isotopes will help us by tracing salinity sources and comparing them to existing data from previous articles and existing databases. In addition, stable water isotope fractionation during brine evaporation is impacted by ion hydration, which results from high salinity values (Clark & Fritz, 1997). This consideration is significant because some of the sampled locations may be subject to the influence of brines. Integrating radiogenic  $^{87}\text{Sr}/^{86}\text{Sr}$  and stable isotopes makes understanding the flow routes in groundwater systems possible (Uliana et al., 2007).



### 1.3 OBJECTIVES

The objectives of this project are: 1) to use water stable isotopes to understand water source, residence time, surface water processes such as mixing and evaporation, and its interaction with groundwater via recharge and discharge, as stable isotope water signatures reflect water source regions' altitude, latitude, and seasonality and 2) to trace with the radiogenic strontium isotope ratios the water sources and salinity sources under different flow conditions along the river courses in the Colorado and Pecos river basins. This study highlights how water-stable isotope ratios and radiogenic strontium isotope ratios provide simple yet significant background information for scientific research and water management strategies (Shand et al., 2009).

## CHAPTER 2: METHODOLOGY

### 2.1 SITE DESCRIPTION

The study sites were situated along the Pecos and Colorado Rivers. Given the large sizes of both river basins, the study was solely concentrated on the Texas section to investigate multiple variations of its lithology, population, and precipitation patterns. Furthermore, existing governmental data obtained from the U.S. Geological Survey (USGS) and Texas Water Development Board (TWDB) were used in the study to address our research questions.

#### *Pecos River and groundwater aquifers*

The Pecos River originates in the southern region of the Sangre de Cristo Mountains in New Mexico and stretches for 1,400 km before joining the Rio Grande at Langtry, Texas (Figure 8) (Yuan & Miyamoto, 2008). The river is subdivided into three basins: the upper basin in Alamo Reservoir, the middle basin in Red Bluff, and the lower basin in Texas. These basins collectively span a total area of 35,000 square miles (Eley, n.d.). Our study focuses on the lower basin area, whose subwatershed is 2,956 sq miles. A digital elevation map (DEM) in Figure 9 of the watershed shows elevation changes from the edge of the Texas watershed to the Gulf of Mexico. Elevation proportionally changes from 2661 meters to 303 meters (at Del Rio, TX) can be observed. The study area is situated within the Chihuahuan desert, characterized by diverse vegetation ranging from desert shrublands at low elevations to conifer woodlands at higher elevations and several species of cactus, yuccas, and agaves. This region is also home to a plethora of fauna, including hundreds of species of amphibians, birds, reptiles, and mammals (“Chihuahuan Desert Ecoregion (U.S. National Park Service),” n.d.). The study area spans seven counties in Texas, including Val Verde, Upton, Crockett, Crane, Pecos, Terrell, and Reagan (Gregory, n.d.). Pecos River receives an average annual rainfall of 19 inches with most rainfalls during the monsoon season, despite

being located mainly in the Chihuahuan Desert area (Gregory, n.d.). The lithology of the area consists of evaporite, sandstones, limestones, shale, and igneous rocks, with remnants of the Permian Basin dating back to 300 million years ago (Gregory, n.d.). Salt formations have been found as deep as 1,000 feet, and the river has been a focus of water management studies due to its high salinity, which affects populations in multiple counties (Gregory, n.d.).

River sampling locations for our study are underlied by the Pecos Valley and Edwards-Trinity Plateau aquifers, which interact with the Pecos River. The Pecos Valley aquifer spans approximately 6,829 square miles and is an unconfined aquifer. Groundwater withdrawal in the area is primarily used for irrigation purposes, with industrial and municipal use accounting for roughly 20% of total water withdrawal (“Pecos Valley Aquifer | Texas Water Development Board,” n.d.). The Edwards-Trinity plateau is also an unconfined aquifer, covering a subsurface area of 3,051 square miles. About 66% of groundwater is utilized for irrigation, while the remaining 30% is allocated for municipal purposes (“Edwards-Trinity (Plateau) Aquifer | Texas Water Development Board,” n.d.-a). The Pecos River watershed is well-known for high salinity complications in its groundwater sources. A study by Dutton, Richter and Kreitler suggested that Permian-formation brine in the area may be mixing with shallow aquifers, increasing salinity levels (Dutton et al., 1989).

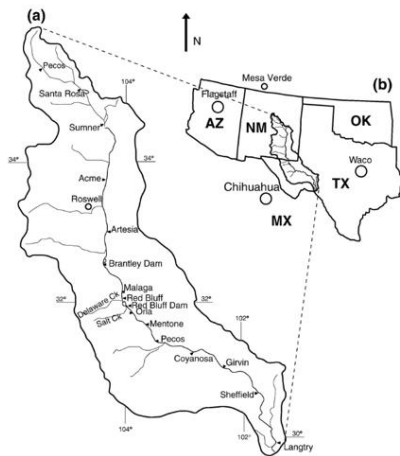


Fig. 1. Map showing the Pecos River drainage basin (a) and its adjacent areas (b).

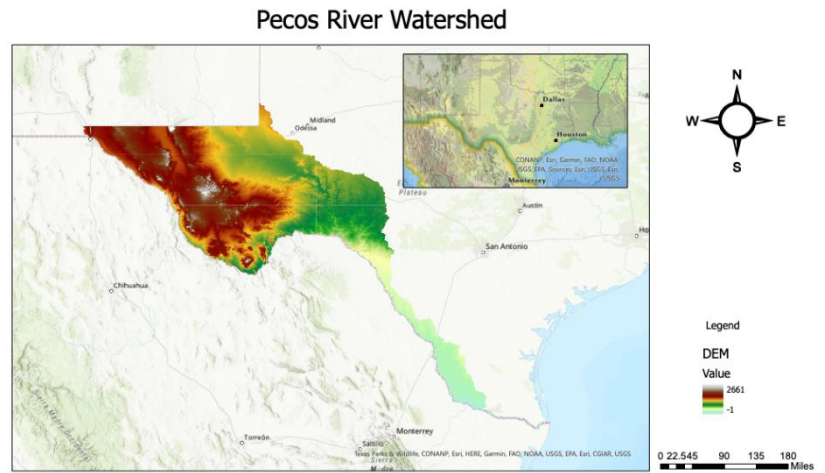


Figure 9: Pecos River watershed with locator map of Texas.

Figure 8: Pecos River drainage system (Yuan & Miyamoto, 2008).

### *Colorado River and groundwater aquifers*

The Colorado River is a major river in Texas, with a length of 600 miles from Dawson County to Matagorda Bay and a drainage area of 40,000 square miles through 20 counties (“River Basins - Colorado River Basin | Texas Water Development Board,” n.d.; “TSHA | Colorado River,” n.d.). The basin is formed by ten smaller basins, with diverse annual average precipitation ranging from 12 to 42 inches (“ColoradoRiverBasinPoster,” n.d.). A digital elevation map (DEM) of the watershed (Figure 10) shows elevation changes from the edge of the watershed to the Gulf of Mexico, with elevation ranging from 1384 meters to 0 meters (sea level).

The geology on the western side of the Colorado River in Texas consists of Quaternary undivided, Blackwater Draw formation, Cretaceous undivided, and Fredericksburg formations. On the eastern side, the geology is diverse, ranging from Washita groups, Jurassic Triassic undivided, Cambrian, Trinity, Austin, Eagle Ford, Woodbine, Yegua formation, Clairborne group, Jackson group, Fleming and Oakville formations, Goliad formation, Lissie formation, and Beaumont formation

(“BEG Maps of Texas - Geology - LibGuides at University of Texas at Austin,” n.d.) The lithology of rivers exhibits variations depending on their location. In the upper watershed, evaporite lithologies dominate, carbonates prevail in the middle portion, and silicate lithologies are found in the lower portion. The vegetation cover along the river also varies, from grassland, mesquite bush, and mesquite shrub/grassland to live oak and post oak woods/forest (“BEG Maps of Texas - Geology - LibGuides at University of Texas at Austin,” n.d.).

### Colorado River Watershed

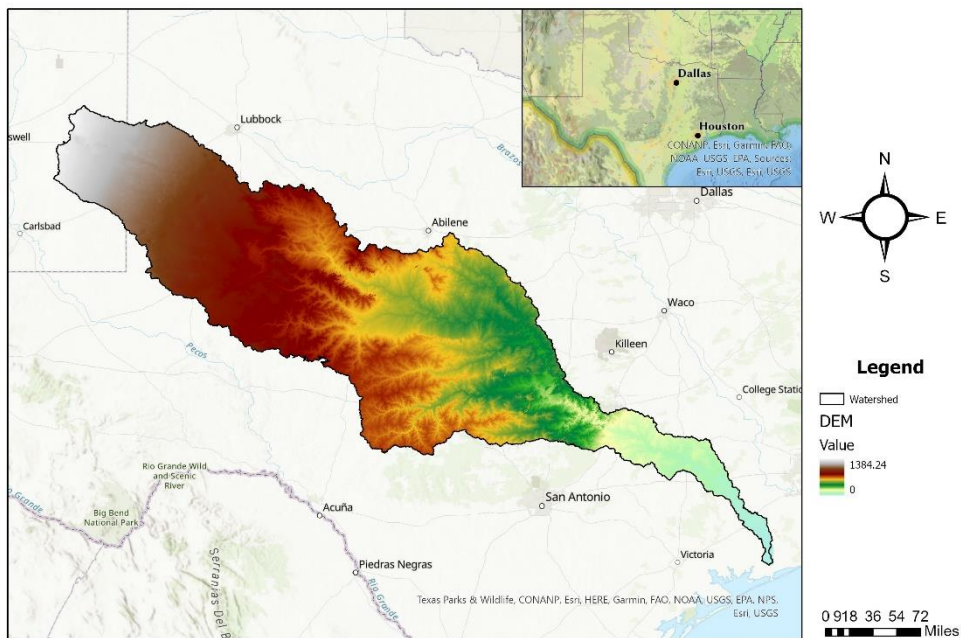


**Figure 10.** DEM of Colorado River Watershed.

Our study sites are underlined by five major/minor aquifers: Edwards-Trinity Plateau, Trinity, Edwards (Balcones Fault Zone), Carrizo-Wilcox, and Gulf Coast (Figure 11). The mostly unconfined Edwards-Trinity Plateau covers a subsurface area of approximately 3,051 square miles. The water in this region contains high amounts of calcium carbonate, and the west side of the area is affected by increased salinity. Municipal and livestock use accounts for 40% of the pumped groundwater, with irrigation purposes making up the remainder (“Edwards-Trinity (Plateau)

Aquifer | Texas Water Development Board,” n.d.-b). Trinity Aquifer is another confined and unconfined aquifer covering a subsurface area of 21,308 square miles. It comprises limestones, sands, and conglomerates, with most pumped groundwater used for municipal purposes (“Trinity Aquifer | Texas Water Development Board,” n.d.). Edwards (Balcones Fault Zone) is a confined and unconfined aquifer with a subsurface area of 2,481 square miles. Though water levels decrease rapidly every year, it is still extensively utilized for irrigation and municipal and recreational activities (“Edwards (Balcones Fault Zone) Aquifer | Texas Water Development Board,” n.d.). Carrizo-Wilcox aquifer is a confined and unconfined aquifer with an extensive subsurface of 25,491 square miles, stretching from the Mexican border to Louisiana. Around forty percent of the pumped groundwater is used for municipal purposes, while the remaining portion is utilized for irrigation (“Carrizo-Wilcox Aquifer | Texas Water Development Board,” n.d.). Lastly, the Gulf Coast aquifer is confined and unconfined and covers a vast area of 41,970 square miles. It is known for high salinity complications due to brines and groundwater pumping (“Gulf Coast Aquifer | Texas Water Development Board,” n.d.).

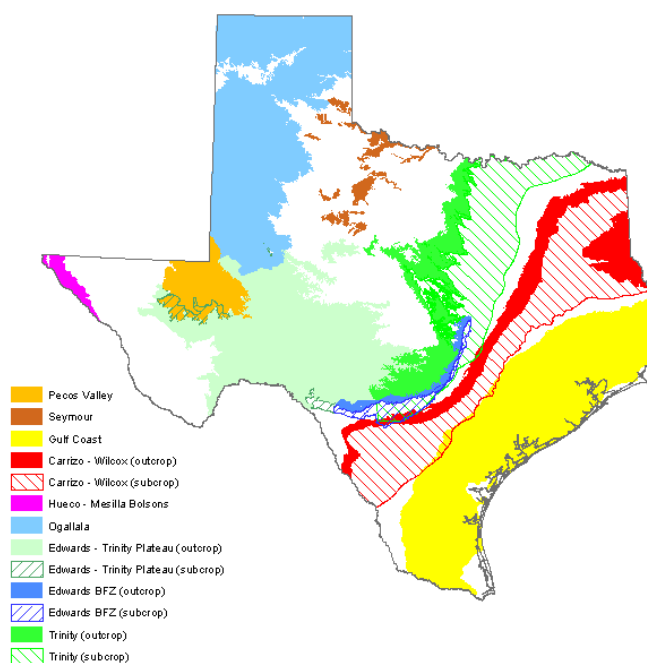


**Figure 11.** Major aquifers map. (“Major Aquifers | Texas Water Development Board,” n.d.)

## 2.2 SAMPLE COLLECTION AND FIELD ANALYSIS

A year-long sample collection was conducted during July 2021, December 2021, and May 2022, during three seasons: July (monsoon), December (dry season), and May (pre-monsoon season). This project aimed to examine the variability of deuterium/hydrogen Oxygen 18/16 ratios and radiogenic strontium isotope ratios, in addition to trace element concentrations. Water samples were obtained from 25 locations along the Colorado (CO) and Pecos (PE) rivers (Figure 12). Most sampling locations were within a USGS (United States Geological Survey) stream gauge station to facilitate logistical coordination and future data reference. Before collection, a bucket and a 1-liter bottle were rinsed three times with stream water. Water samples were then collected using a bucket and transferred to the rinsed 1-liter HDPE Nalgene bottle. Water samples were stored in a cooler for subsequent laboratory analysis. In-situ field measurements were conducted using a

calibrated YSI ProQuatro Multiparameter Meter Field to obtain dissolved oxygen, electric conductivity, total dissolved solids (TDS), pH, oxidation-reduction potential (ORP), and temperature values. Alkalinity was measured in situ using the LaMotte field alkalinity test kit. Before filtration, a syringe was rinsed three times using stream water, and the resulting sample was filtered using a 0.45 $\mu$ m Whatman syringe filter. Subsequently, a 5 mL filtered water sample was mixed with a BCG-MR indicator tablet in a glass vial until it dissolved. Then, a CaCO<sub>3</sub> alkalinity titrator was added drop by drop using a 0-200 ppm syringe, with the titration ending when the sample turned violet.

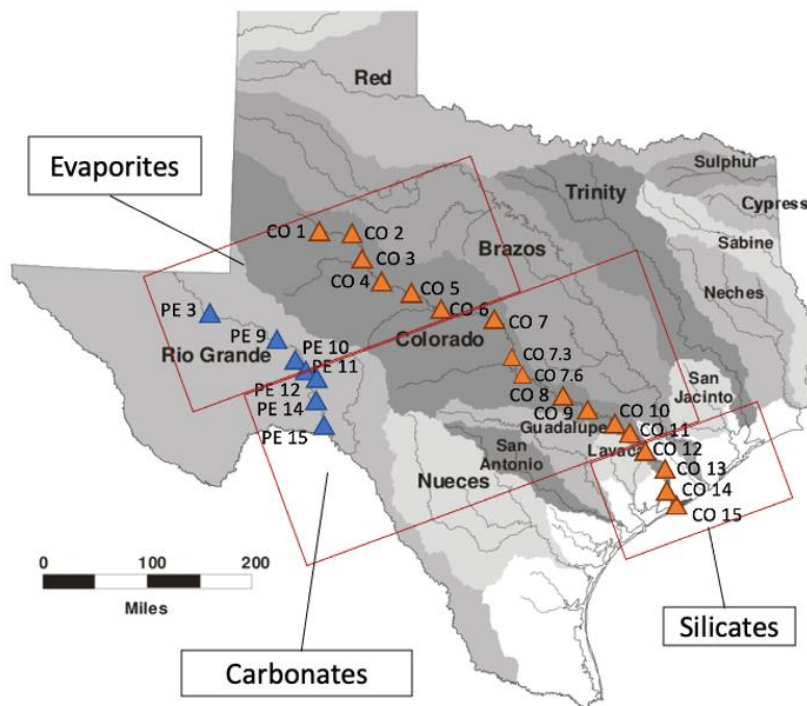


**Figure 12.** Pecos and Colorado rivers and basins with numbered sampling locations (Ward, n.d.).



## 2.3 SAMPLING – RELATED LIMITATIONS

Some limitations were imposed on the results by the sampling time. The results are delimited by the sampling time, potentially influencing the origins and magnitudes of trace elements and salinity levels. This means that the rivers flow conditions could have exhibited variability across different times of the day. The logistical requirement to cover multiple sampling locations dedicated an entire day. Predominantly, the collection of samples commenced between 8 a.m. and 6 p.m. It is noteworthy to emphasize the substantial travel involvement to reach distinct sites, often accompanied by challenges accessing sampling points.

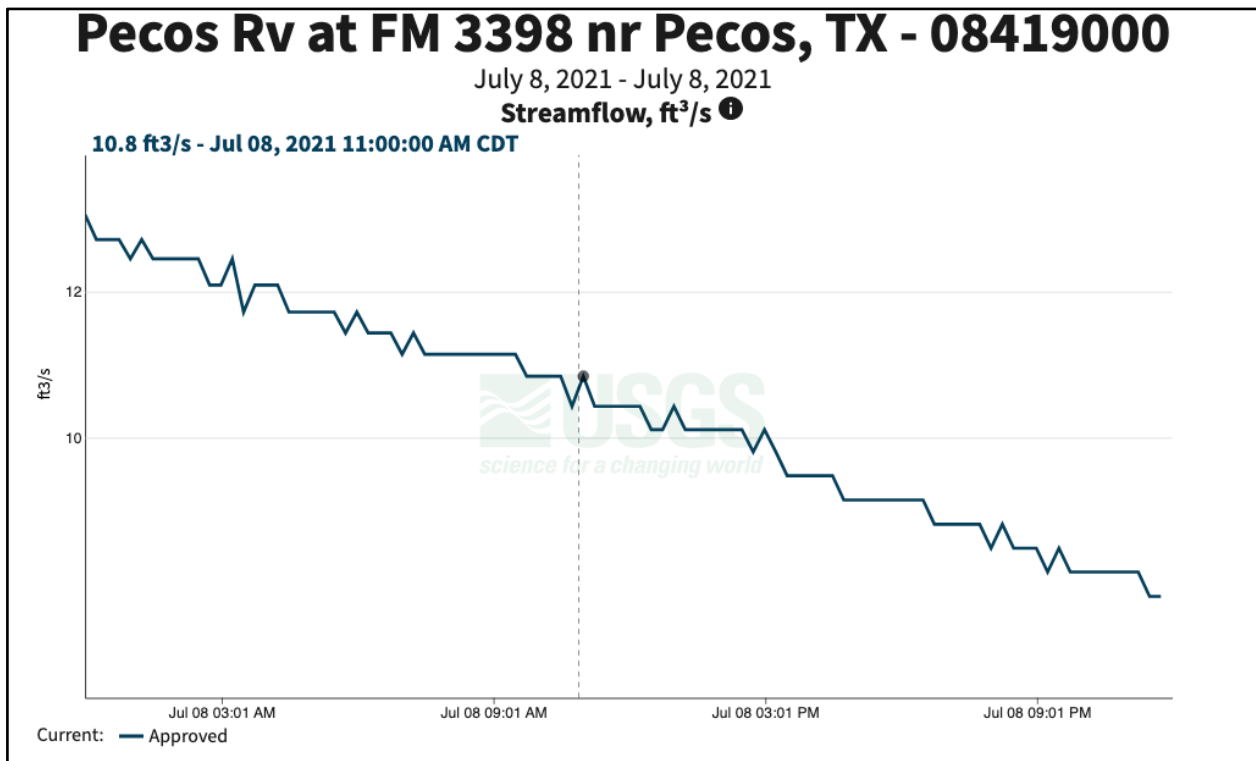


**Figure 13.** Streamflow versus time graph in ft<sup>3</sup>/s of PE3.

Figure 13 illustrates a flow duration curve, specifically delineating the discharge characteristics at the initial sampling point along the Pecos River. The temporal evolution of discharge levels over the day is noticeable within this description. Sampling for this site was at approximately 11 a.m.; nevertheless, it is essential to emphasize the considerable change in the

river discharge throughout the day. This could have influenced our sample values, but it is a limitation we cannot control. It is essential to mention that our designated sampling locations are notably separated and conducting constant and daily field sampling was not feasible. Sampling collection is labor-intensive, and this was the best way to interpret the river's health. For future analyses, a more uniform temporal framework for river sampling can be an excellent opportunity to understand the river changes between multiple seasons. A complete year-long analysis can respond to more questions on this topic. Such an approach would provide valuable insights into the extent of temporal variability exhibited by the river, particularly across the delineated seasonal periods under study.

## 2.4 LABORATORY ANALYSIS

Water samples were filtered using an electric pump and 0.45  $\mu\text{m}$  membrane filter from Thermo Scientific to separate suspended particles and large colloids from stream water. Filtered water was transferred to two 250 mL HDPE Nalgene bottles (acidified and non-acidified). Three drops of concentrated  $\text{HNO}_3$  were added to acidify samples for  $^{87}\text{Sr}/^{86}\text{Sr}$  and trace metals analysis. The non-acidified samples were stored in a refrigerator for stable isotope analysis. Used filters are stored in a plastic bag for future analysis. Stream water alkalinity was analyzed using a Mettler Toledo DL 15 Endpoint Titrator. The instrument was calibrated using two-point (4 and 7) pH solutions and 13 mmol  $\text{HCl}$ . Three  $\text{NaHCO}_3$  standards are weighted and zeroed to calibrate the titrator. Once there is a consistent result, water samples can be analyzed.

## 2.5 WATER STABLE ISOTOPES RATIO ANALYSIS

Since the water samples have high salinity levels, a multiple-step cryogenic extraction was assembled to remove salts from the sample. The extraction method utilized has a similar procedure to Gardea (2021). Materials include an Edwards Vacuum Pump, Fisherbrand Isotemp Digital Block Heaters, Thermos Stainless steel container, PolyScience immersion probe cooler, and glass

vials (Figure 13). Before initiating the extraction, each sample test tube is examined to avoid leaks by tightly securing each part and assuring a vacuum effect. The test tube has a cock valve, screw joints, and two glass tubes (Scholarworks@utep & Gardea, n.d.). The cryogenic extraction involves introducing one microliter of sample water into a test tube and freezing using isopropyl alcohol at  $-50^{\circ}\text{C}$ . The frozen sample is connected to Edwards Vacuum Pump to remove air pressure until 0 or 1 psi is reached. When a vacuum effect is completed, the frozen water sample is left over a hot tray at  $100^{\circ}\text{C}$  to evaporate and generate a thermal shock. Due to the change in pressure and temperature, water evaporates and moves to the colder region; salts remain on the hot plate side (Figure 12). Once complete, samples are left to thaw, transferred to small plastic or glass vials (Figure 13, E), sealed with parafilm, and stored in the refrigerator for hydrogen and oxygen analysis. Due to the tendency of water to condense upon heating, the vacuum distillation method is preferred for its high efficiency and avoiding isotopic fractionation (Scholarworks@utep & Gardea, n.d.). Samples were analyzed for Deuterium/hydrogen and Oxygen 18/16 ratios with a Picarro L2130-*i* Isotope and Gas Concentration Analyzer (Figure 15).

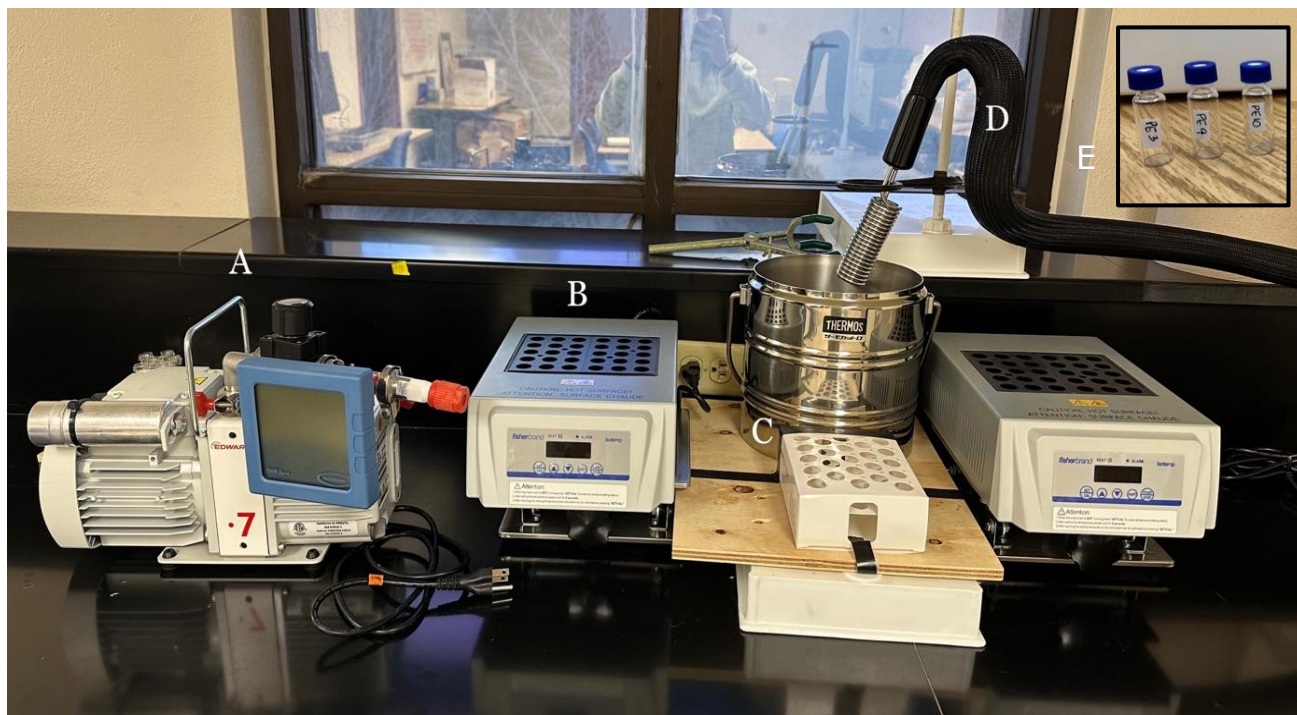


**Figure 13.** Cryogenic vacuum extraction setup. A) Edwards Vacuum Pump, B) Fisherbrand Isotemp Digital Block Heaters, C) Thermos Stainless steel container, D) PolyScience immersion probe cooler, E) Glass vials.

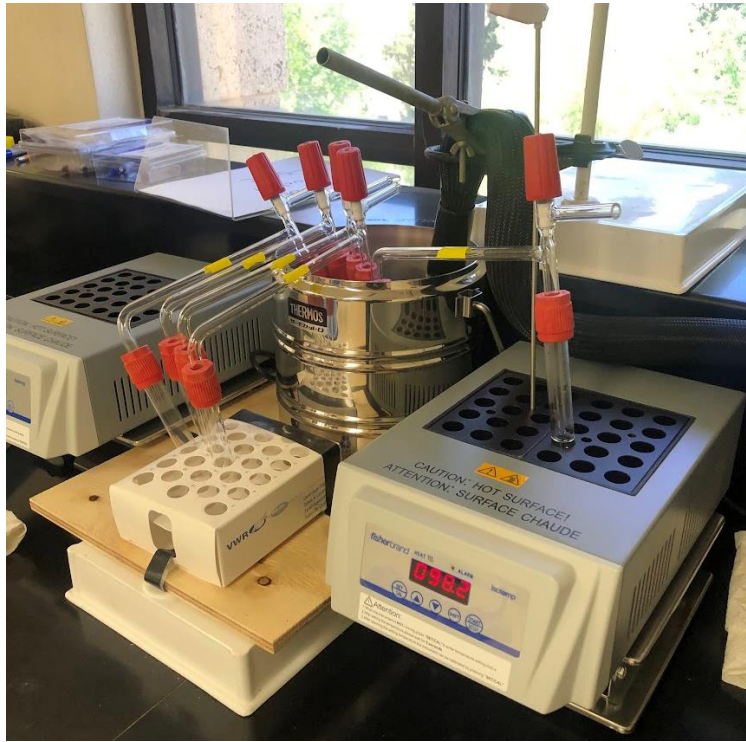


**Figure 14.** Cryogenic river water extraction: Glass test tubes with frozen samples at  $-50^{\circ}\text{C}$  in a Thermos stainless steel container. In addition to evaporating samples in Fisherbrand Isotemp Digital Block Heaters.



**Figure 15.** Cavity Ringdown Spectrometer Picarro L2130-i Isotope and Gas Concentration Analyzer

The Picarro L2130-i Isotope and Gas Concentration Analyzer were used for the isotopic measurements (Figure 15). The analyses include zero, mid, and depleted isotope standards at the beginning, then the water samples to be analyzed in order. Once the autosampler is calibrated and gas has been released, it is ready to be used.

2.6 QUALITY ASSURANCE QUALITY CONTROL ON STABLE ISOTOPE RATIO  
ANALYSIS

Table 1. Reference values from Picarro Chemcorrect.

Name	Reference Values		$\Delta^{18}\text{O}$	stdv	$\Delta\text{H}$	stdv
	$\Delta^{18}\text{O}$	$\Delta\text{H}$				
Zero	0.3	1.8 (0.9-2.7)	0.56	$\pm 0.42$	3.15	$\pm 2.25$
Mid	-20.6	-159 (157.7-160.3)	-20.29	$\pm 0.28$	-157.82	$\pm 1.58$
Depleted	-29.6	-235 (233.2-236.8)	-29.73	$\pm 0.09$	-236.30	$\pm 1.48$

A quality assurance/quality control calculation was created using Picarro’s Chemcorrect document for each time the samples were run for the stable isotope ratios. To create this, the average was used from all samples. In addition, a reference value from Picarro instructional manual was used to understand the limits (standards) on each sample run.

***87Sr/86Sr Isotope Analysis***

The acidified samples, utilizing pure hydrochloric acid (HCl), were subjected to analysis for the isotopic ratio of 87Sr/86Sr. This method involved evaporating 7 ml of the sample water in Teflon beakers, which were hydrated with 3.5 N nitric acid (HNO3) and isolating the samples through Sr-Spec resin (Garcia et al., 2021). The separated samples were then quantified for the 87Sr/86Sr ratio using a multi-collector inductively coupled plasma mass spectrometer (MC-ICP-MS), with the NIST Standard Reference Material 987 serving as the bracketing solution for calibration purposes (Garcia et al., 2021).

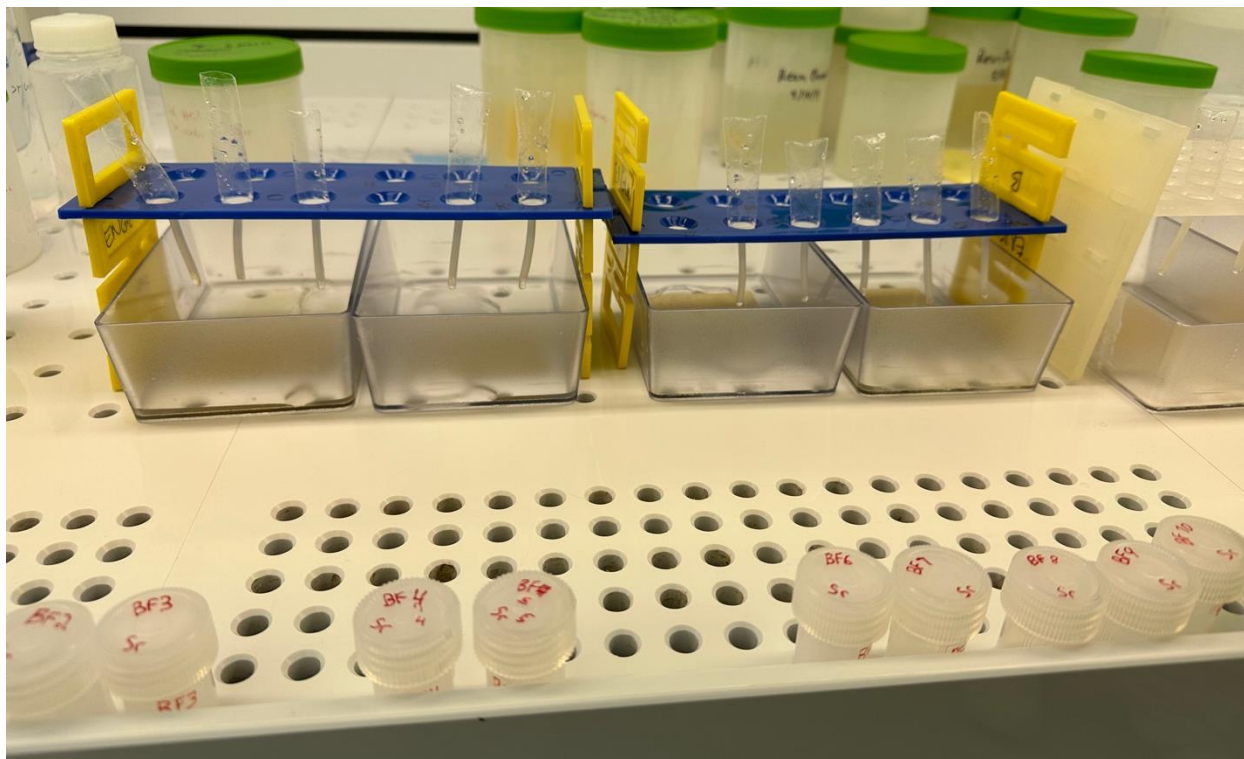


**Figure 16.** Laboratory analysis for Sr isotopes. Plastic columns with strontium resin and sample.

Multiple elements were selected to be included in our study. The elements include Arsenic (As), Cadmium (Cd), Lead (Pb), Boron (B), Vanadium (V). Trace elements analysis was completed using a Thermo Fisher Scientific iCAP RQ ICP-MS. A water standard (NIST 1640a) was used to evaluate precision on the method (Garcia et al., 2021).



## CHAPTER 3: RESULTS

### 3.1 WATER STABLE ISOTOPES: $\delta^{18}\text{O}$ and $\delta\text{D}$ ratios

Water samples were collected from various locations along the Pecos and Colorado rivers for three different seasons, July 2021 (monsoon), December 2021 (dry), and May 2022 (pre-monsoon), to study and understand seasonal and spatial variabilities. There was a total of eight sample locations from the Pecos River (PE) (Figure 17) and seventeen sample locations from the Colorado River (CO) (Figure 18). Pecos River only has data from July and December 2021 and no samples for May 2022 when the sample locations were totally dry. The sample locations within both watersheds were divided into 2 or 3 categories. **Upper watershed:** PE (3, 9, 10), CO (1-6), **Middle watershed:** PE (11-15.5), CO (7-11), and **Lower watershed:** CO (12-15).

For all the Pecos River samples,  $\delta^2\text{H}$  from Pecos River have a range of -40 to -3 ‰, while  $\delta^{18}\text{O}$  range from -9 to +3 ‰.  $\delta^2\text{H}$  for the upper region ranges from -38.04 to -3.43‰ and the middle region -39.66 to -14.85‰. The upper region for  $\delta^{18}\text{O}$  ranges from -4.45 to -8.40‰ and the middle portion -5.53 to -1.82‰. Samples PE 11 to PE 15.5 for both July and December as well as PE 10 and PE 3 from July are closer to the Global Meteoric Water Line (GMWL) indicating precipitation signature (Figure 17). PE 3 and PE 10 samples from December and PE 9 samples are further away from the GMWL, which may be related to decreased precipitation contribution and increased brine contribution during dry seasons. In general, the upper portion of the watershed exhibits a more significant separation from the Global Meteoric Water Line (GMWL) and the samples from the middle portion of the watershed align more closely with the GMWL.

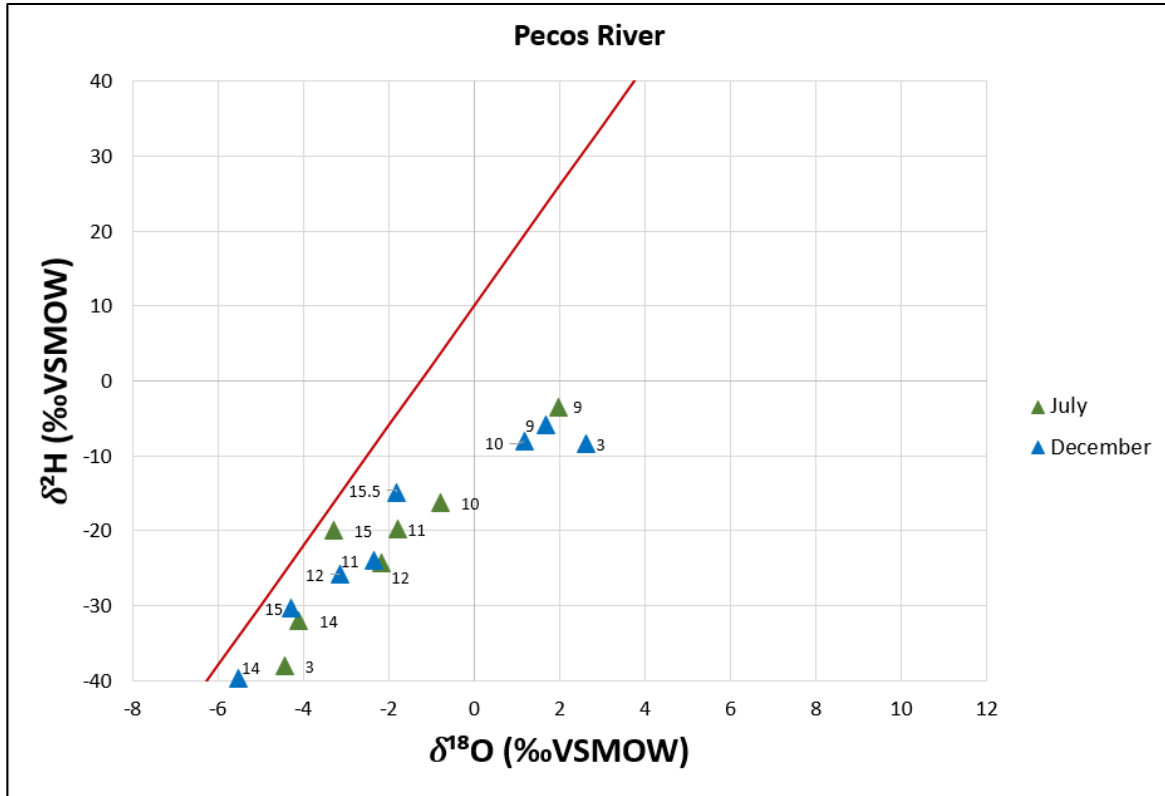


**Figure 17.**  $\delta^2\text{H}$  and  $\delta^{18}\text{O}$  (‰VSMOW) plot all eight sample sites from July 2021 to December 2021. The Global Meteoric Water Line (GMWL) is a standard value  $\delta^2\text{H} = 8 * \delta^{18}\text{O} + 10$ ‰ SMOW.

Most samples in  $\delta^2\text{H}$  from the Colorado River have a range of -40 to +10 ‰, while  $\delta^{18}\text{O}$  range from -6.3 to +3 ‰, except for sample CO 1 that shows extreme high values for  $\delta^2\text{H}$  and  $\delta^{18}\text{O}$ . Water stable isotope ratios of the Colorado River samples vary significantly from the headwater source region to its end in the Gulf of Mexico. The upper portion of the watershed (CO1 to CO6) exhibits large separation from the Global Meteoric Water Line (GMWL) across multiple seasons, contrasting with the middle and lower parts of the river (Figure 18). The samples in the middle portion (CO7-CO11) tend to align closely with the GMWL, with occasional separations observed during the pre-monsoon season. Similarly, the lower part of the river (CO12-CO15) shows proximity to the GMWL, with some variations also followed during the pre-monsoon season.

There is higher rainfall isotope signature during July and December (plotting along/close to the GMWL) in the middle and lower areas of the river. On the contrary, May samples are further away from the line due to a lower precipitation value or evaporation. Samples separated from the GMWL may represent mixing or evaporation, as it was explained in Figure 6. In addition, sample CO 6, both from July and December, deviated from the rest of the points that are close to the GMWL. Lastly, sample CO 1 (May) is highly separated from the rest of the data points.

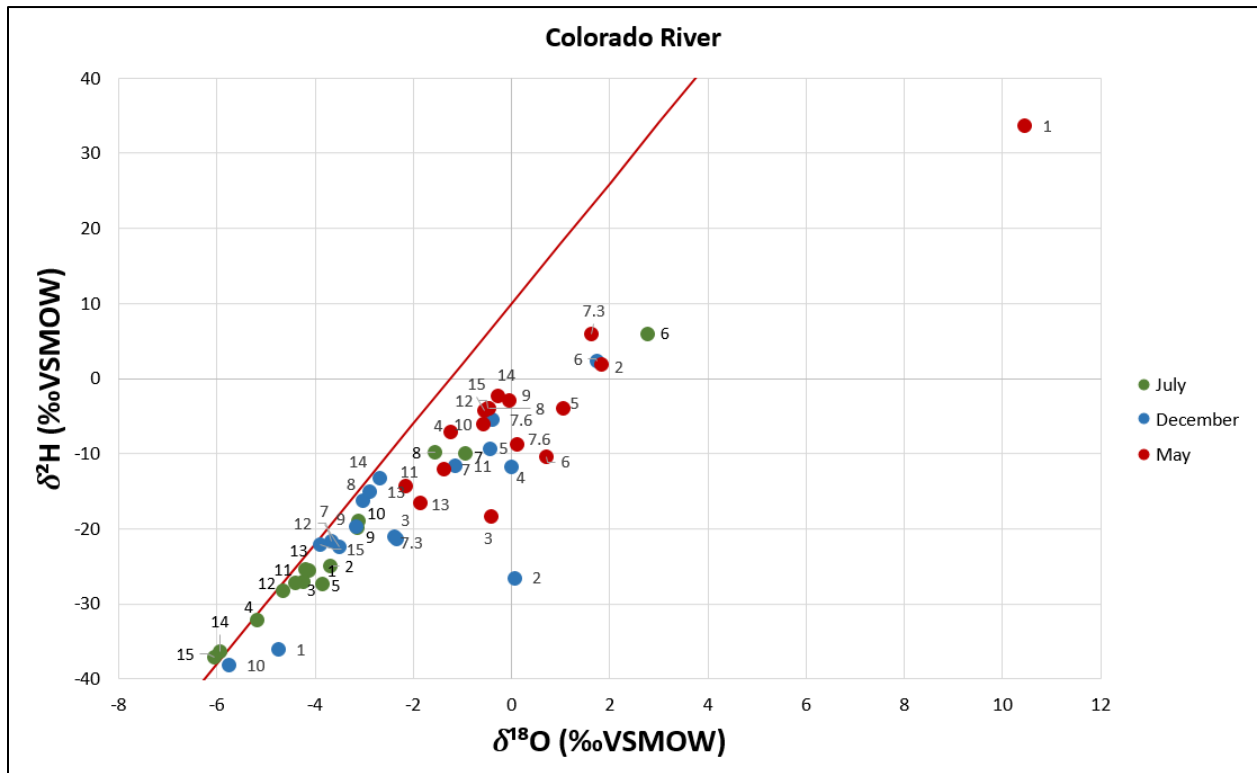


**Figure 18.**  $\delta^2\text{H}$  and  $\delta^{18}\text{O}$  (‰ VSMOW) plot of all seventeen sample sites from July 2021, December 2021, and May 2022. The Global Meteoric Water Line (GMWL) is a standard value  $\delta^2\text{H} = 8 * \delta^{18}\text{O} + 10$  ‰ SMOW.

### 3.2. Electrical conductivity values.

High electrical conductivity (EC) of ~10,000 to 30,000  $\mu\text{s}/\text{cm}$  is observed in the Pecos River in sites PE3, PE9, PE10, and PE11, which are in the upper region of the river (Figure 19) both in July and December. In addition, the Wolfcamp formation, which has a brine influence, is located near

sample sites PE 3 and PE 9. It is essential to mention that values do not vary as much between seasons, only with site 3, which decreased from 10,000  $\mu\text{s}/\text{cm}$  in winter to 2780  $\mu\text{s}/\text{cm}$  in the summertime. Generally, as we sampled the river flowing into the Rio Grande at Del Rio, TX, EC decreased from  $\sim 10000$  to 800  $\mu\text{s}/\text{cm}$  from PE 12 to PE15.

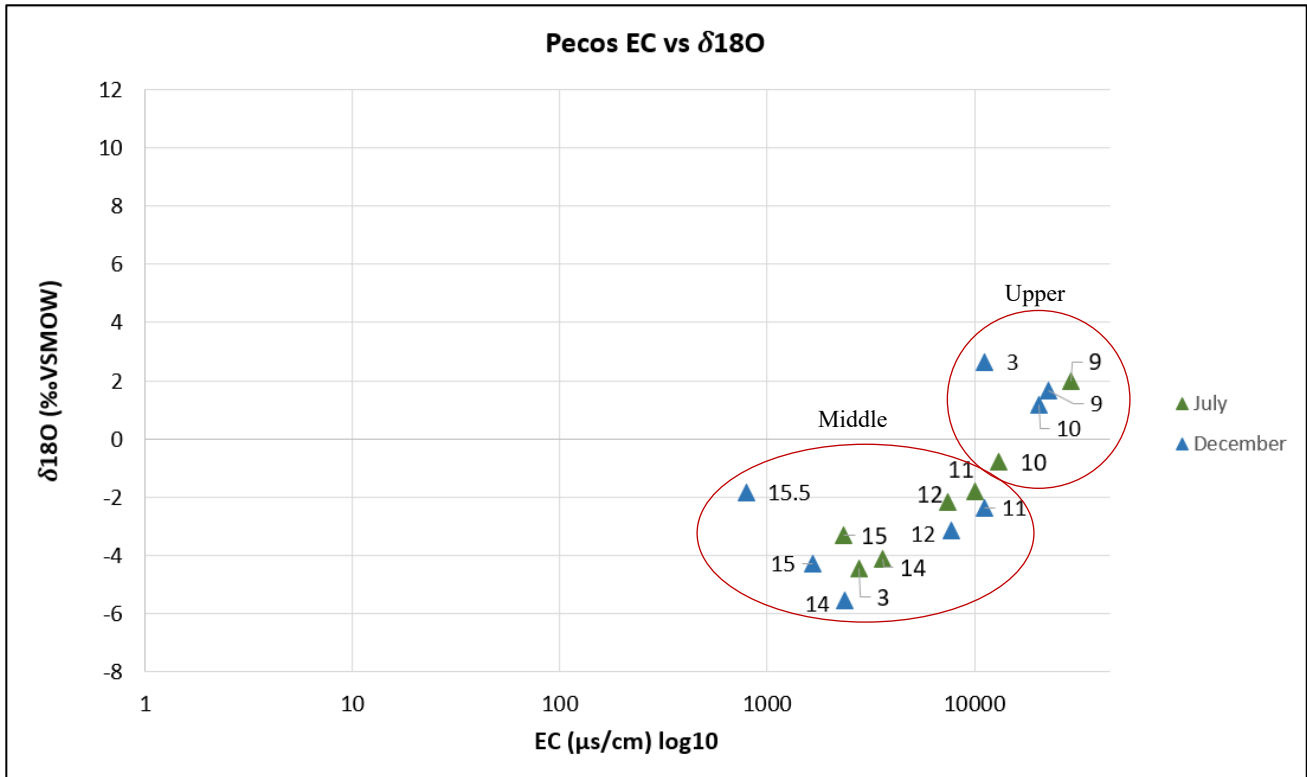


**Figure 19.**  $\delta^{18}\text{O}$  and Electrical Conductivity (EC) plot of all eight sample sites from July 2021 and December 2021. EC concentration is higher with samples 3, 9, and 10.

High electrical conductivity (EC) of  $\sim 1500$  to  $44,000 \mu\text{s}/\text{cm}$  (representing about 10% of seawater salinity) is observed in sites CO1 to CO6 in the Colorado River. These are in the upper region of the river (Figure 20), both in May and December. On the contrary, the same samples in July have lower EC values. The middle section of the river (CO 7-11) has EC values  $\sim 400$  to  $1000 \mu\text{s}/\text{cm}$  with an overlap with the lower section of the river. Lastly, the lower portion (CO 12-15), EC, ranges from  $\sim 190$  to  $999 \mu\text{s}/\text{cm}$ . Some outliers are present such as CO15 in May, which is highly

concentrated compared to the other seasons. As we sampled the river flowing into the Gulf of Mexico, EC decreased to ~100 to 1000  $\mu\text{s}/\text{cm}$  (>1000 is considered freshwater).

EC values from Pecos and Colorado Rivers show positive correlations with  $\delta^{18}\text{O}$  values (Figures 19 and 20), with more scatterings in samples from the Colorado Rivers compared to the Pecos Rivers.

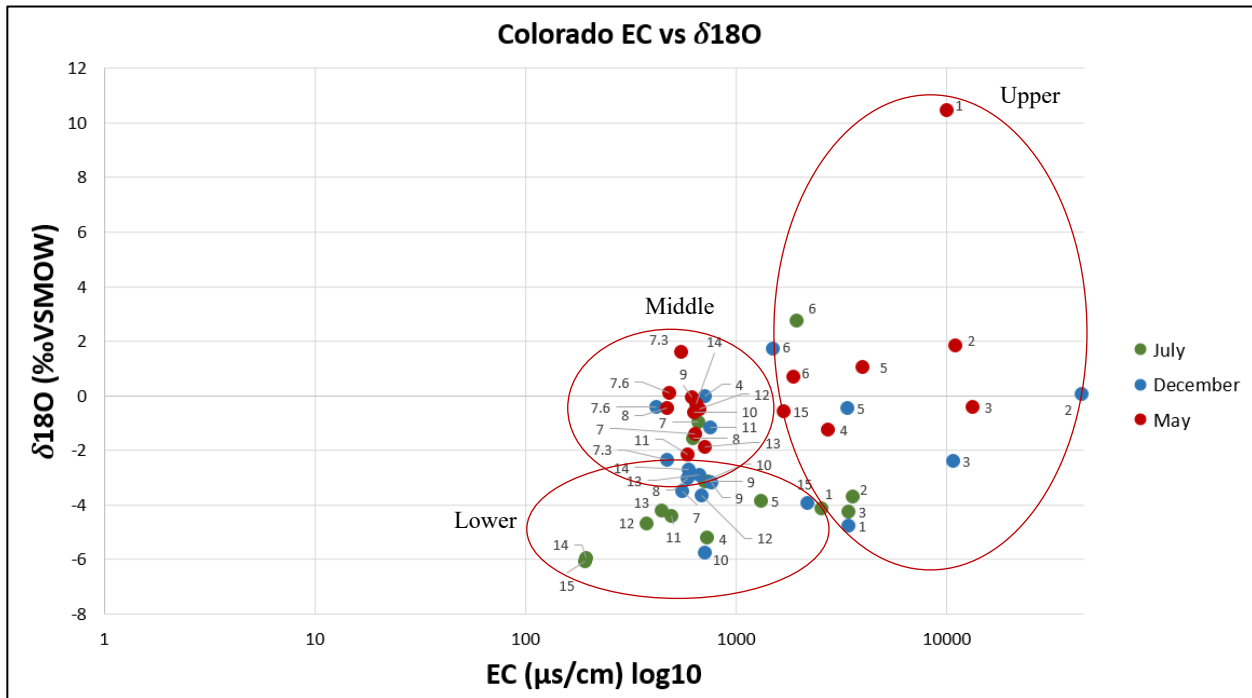


**Figure 20.**  $\delta^{18}\text{O}$  and Electrical Conductivity (EC) plot of all seventeen sample sites from July 2021, December 2021, and May 2022.

### 3.3. $^{87}\text{Sr}/^{86}\text{Sr}$ ISOTOPES RATIOS AND CORRELATION WITH $\delta^{18}\text{O}$ RATIOS

The  $^{87}\text{Sr}/^{86}\text{Sr}$  ratios observed in the Pecos River range from 0.7075 to 0.7085, while the  $\delta^{18}\text{O}$  values vary from -6 to +4 ‰ (Figure 21). The upper part of the watershed (PE3, PE9-PE11) predominantly falls within the 0 to 4 ‰ range for  $\delta^{18}\text{O}$ , except for sample PE 3 in July. In contrast, the middle portion of the river (PE12-PE15) is mainly concentrated within a range of -6 to 3 ‰ for  $\delta^{18}\text{O}$ . The July sample collected at site PE 3 exhibits a low  $^{87}\text{Sr}/^{86}\text{Sr}$  ratio and a low  $\delta^{18}\text{O}$  value, potentially due to the rainy season and precipitation isotope signature. On the other hand, the December sample obtained at site PE 3 appears to be significantly distinct from the other data points, displaying a low  $^{87}\text{Sr}/^{86}\text{Sr}$  ratio but a high  $\delta^{18}\text{O}$  value. Notably, the group of samples below site 3 (i.e., samples 9, 10, 11, and 14) demonstrates higher Sr ratios in both seasons, while the remaining samples exhibit a range of low  $\delta^{18}\text{O}$  values. It is noted that the spatial and seasonal variability of  $^{87}\text{Sr}/^{86}\text{Sr}$  ratios is much smaller than the  $\delta^{18}\text{O}$  ratios in Pecos River.

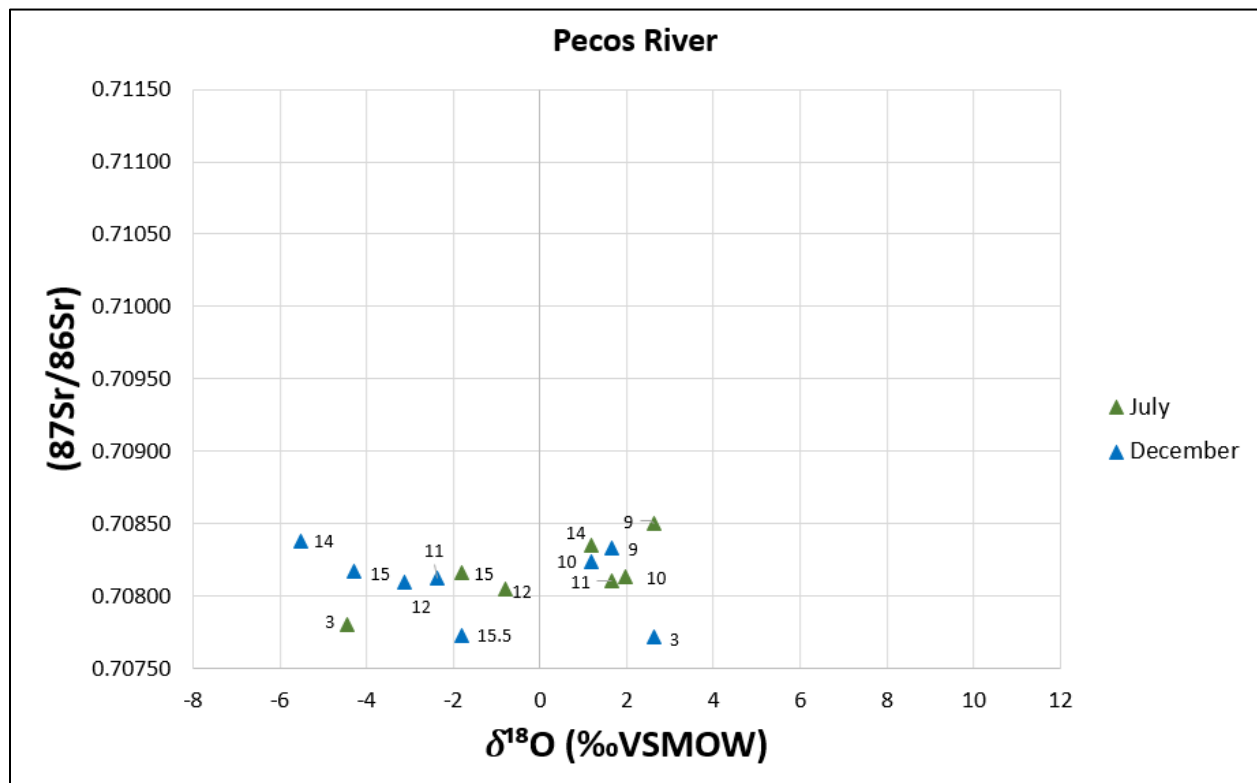


**Figure 21.**  $^{87}\text{Sr}/^{86}\text{Sr}$  and  $\delta^{18}\text{O}$  isotopic ratio plot of all eight sample sites from July 2021 and December 2021.

The  $^{87}\text{Sr}/^{86}\text{Sr}$  ratios observed in the Colorado River range from 0.7080 to 0.7110, while the  $\delta^{18}\text{O}$  values vary from -6.5 to 3 ‰, with an outlier on site CO1 (Figure 22). Strontium in the upper region range from 0.7083-0.7093, middle 0.7084-0.7097, and lower 0.7085-0.7095. However, certain exceptions, namely samples CO 7.3 and CO 7.6, display notable radiogenic characteristics due to their positioning within the Llano Uplift (0.7098-0.7109). Sites 7.3 and 7.6 appear unaffected by seasonal variations.

The upper portion of the river (CO1 to CO6) displays a large degree of scatters across different sections of the plot, depending on the season. Site CO1 exhibited the most drastic separation in May from the other samples. Furthermore, during May, the samples tend to be concentrated within the range of -2 to 2 ‰ for  $\delta^{18}\text{O}$  ratios. In the middle portion of the watershed (CO7 to CO11), most samples fall within the range of -5 to 0 ‰ for  $\delta^{18}\text{O}$  ratios, with only a few outliers at 7.6 ‰. Lastly, the lower section of the river (CO12-CO15) demonstrates a concentration of samples within the range of -6 to 0 ‰. However, some May samples remain within the middle region of the plot. Most samples have  $^{87}\text{Sr}/^{86}\text{Sr}$  ratios with less variability compared to the  $\delta^{18}\text{O}$  values, which exhibits higher precipitation contributions across three seasons.

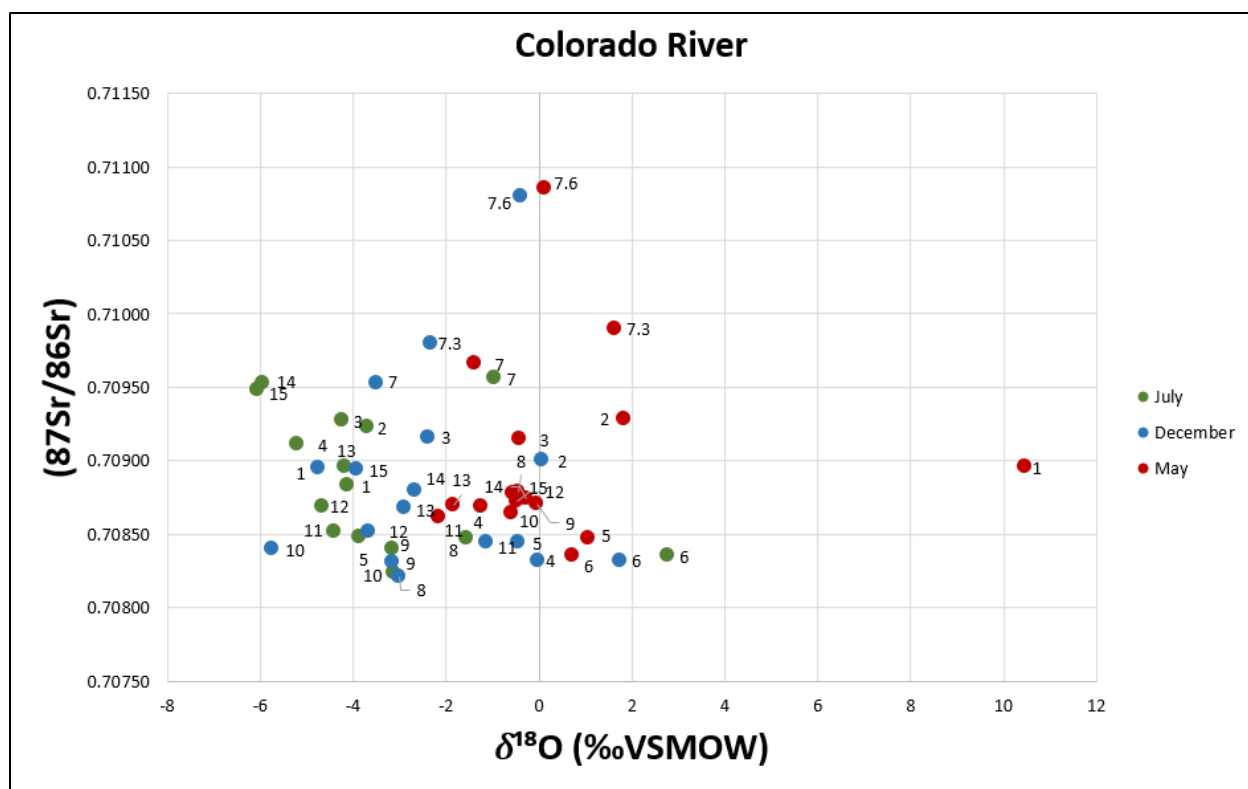


**Figure 22.**  $^{87}\text{Sr}/^{86}\text{Sr}$  and  $\delta^{18}\text{O}$  isotopic ratio plot of all seventeen sample sites from July 2021, December 2021, and May 2022.

Plotting  $^{87}\text{Sr}/^{86}\text{Sr}$  ratios with  $1/\text{EC}$  (Electrical Conductivity) or  $1/\text{TDS}$  (Total Dissolved Solids) is a reliable method for understanding mixing patterns. In Figure 23, low  $1/\text{EC}$  values are associated with high  $^{87}\text{Sr}/^{86}\text{Sr}$  values. Most values in the upper region of the river exhibit proximity to zero in  $1/\text{EC}$  values (very high EC values). In contrast, the middle portion displays a slightly greater separation. Sample 15.5 is significantly separated from all other samples within the middle region.



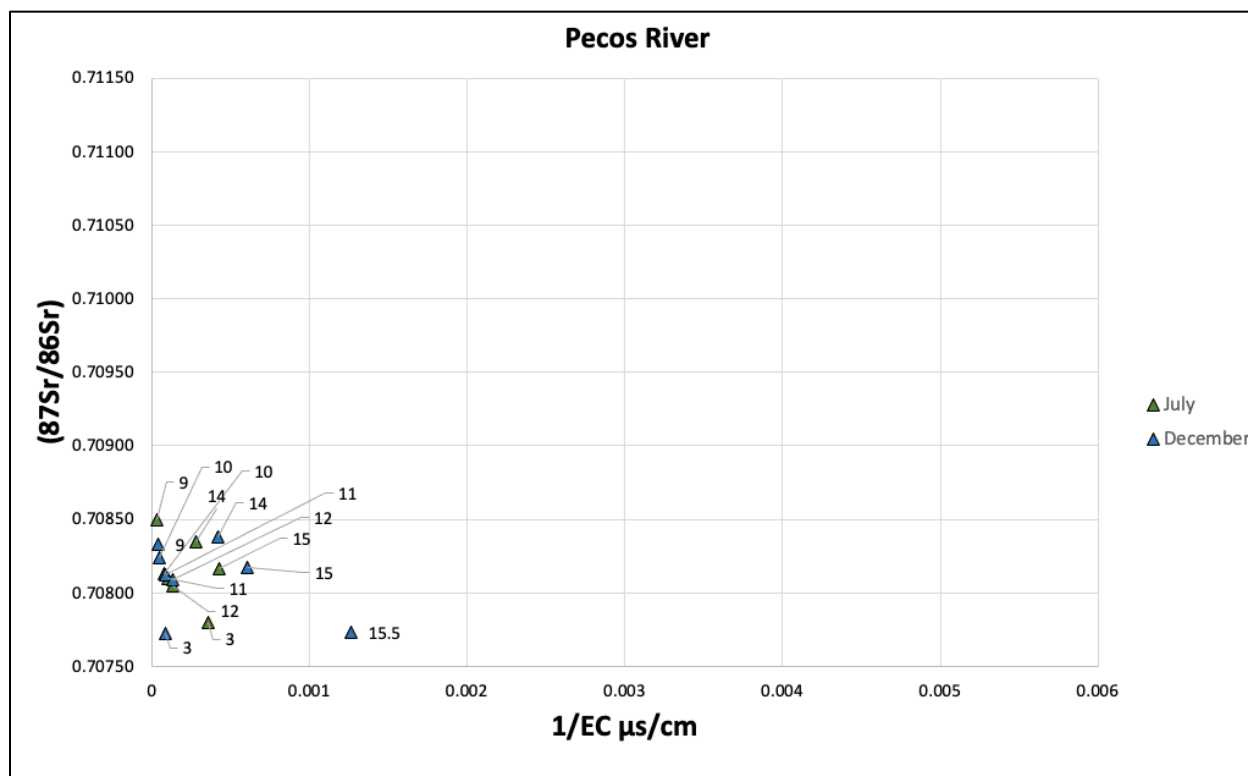


**Figure 23.**  $^{87}\text{Sr}/^{86}\text{Sr}$  and  $1/\text{Electrical Conductivity}$  plot of all eight sample sites from July 2021 and December 2021.

Similarly, Colorado River shows low  $1/\text{EC}$  values but high strontium  $^{87}\text{Sr}/^{86}\text{Sr}$  ratios (Figure 24). The plot demonstrates a more distinct separation from different portions of the river. In the upper region, most samples consistently fall within the 0 to 0.001 ( $1/\text{EC}$   $\mu\text{s}/\text{cm}$ ) range across all seasons. The middle portion of the river shows a relatively narrower range of conductivity values, but with high variable  $^{87}\text{Sr}/^{86}\text{Sr}$  ratios, primarily between 0.7085 and 0.7110. However, sample CO 7.6 is separated from the other samples within this region. In the lower region, the conductivity values cluster closely to those observed in the middle portion. However, two outliers are observed in samples CO 14 and CO 15 in December.

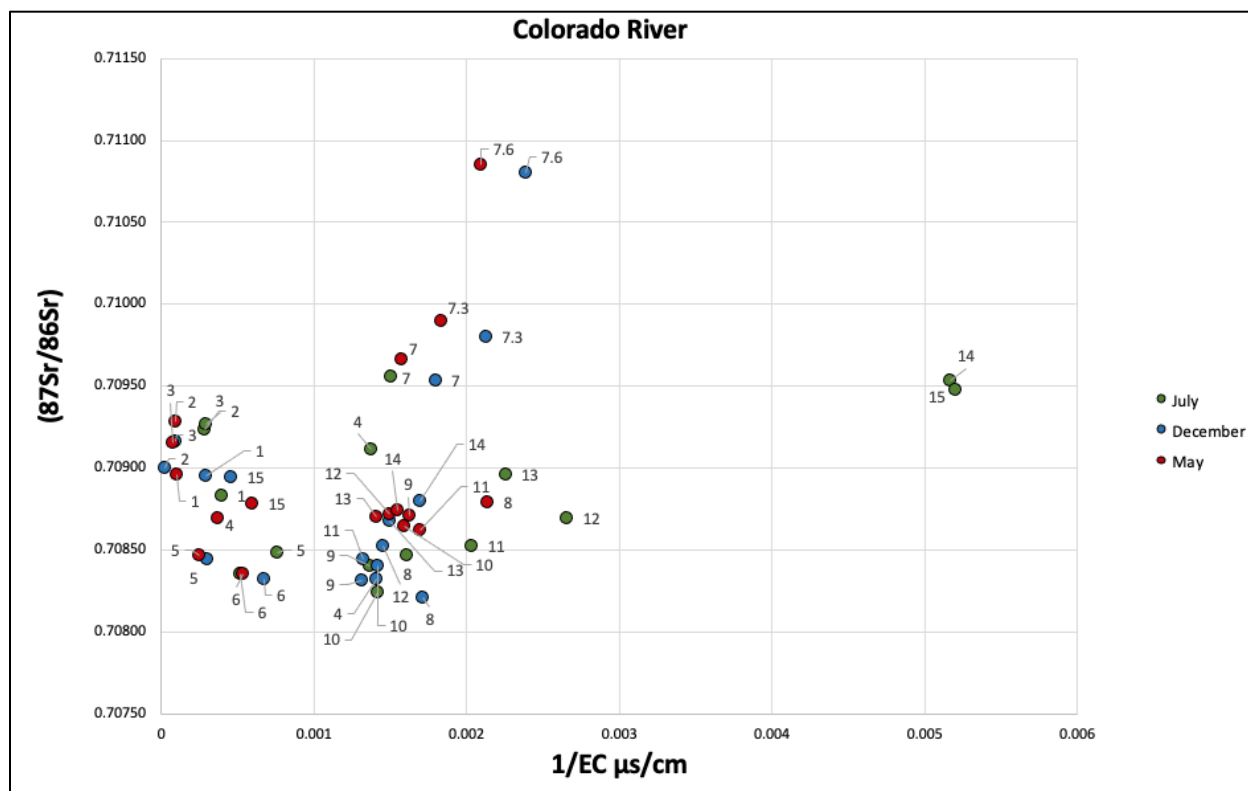


**Figure 24.**  $^{87}\text{Sr}/^{86}\text{Sr}$  and  $1/\text{Electrical Conductivity}$  plot of all seventeen sample sites from July 2021, December 2021, and May 2022.

Most samples in Pecos River exhibit a notable trend characterized by a high  $1/^{88}\text{Sr}$  concentration and a lower  $^{87}\text{Sr}/^{86}\text{Sr}$  ratio (Figure 25). Moreover, the July and December samples at site PE 3 demonstrate high Sr concentrations with lower  $^{87}\text{Sr}/^{86}\text{Sr}$  ratios. Notably, sample PE 15.5, located in the lower portion of the Pecos River, displays a combination of high Sr concentration and a comparatively low  $^{87}\text{Sr}/^{86}\text{Sr}$  ratio. This observation highlights the significance of considering the spatial distribution and hydrological dynamics in interpreting Sr concentration and isotopic ratios within the studied system.

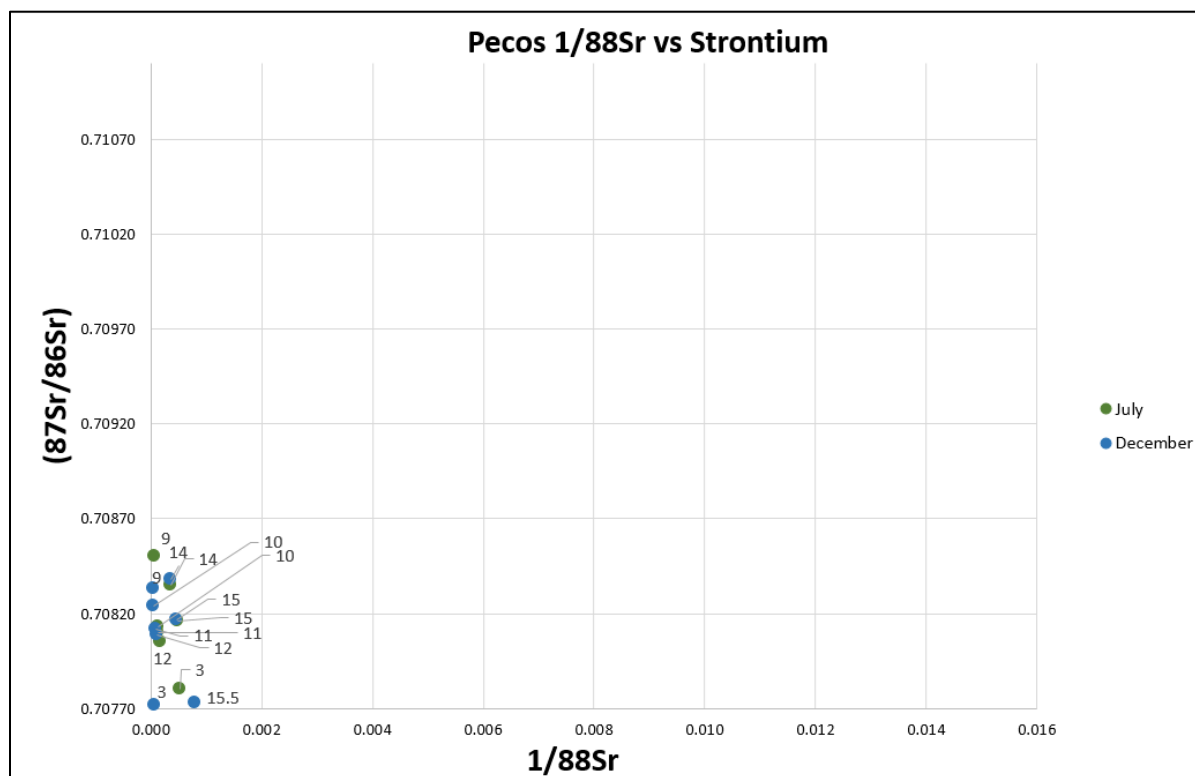


**Figure 25.**  $^{87}\text{Sr}/^{86}\text{Sr}$  ratio vs  $1/^{88}\text{Sr}$  illustrating mixing trends among multiple data points. The relationship between these isotopic ratios provides insights into the mixing processes within the studied system. Points on  $1/^{88}\text{Sr}$  closer to 0 represent a high concentration.

In Colorado river, samples from CO1 to CO6 exhibit a consistent pattern characterized by an increasing trend in  $1/^{88}\text{Sr}$  concentration and a corresponding decrease in Sr ratio as the river flows into the middle portion. Conversely, samples 7 to 7.6 display a different mixing trend, indicated by an  $^{87}\text{Sr}/^{86}\text{Sr}$  ratio increase with higher  $1/^{88}\text{Sr}$  concentrations within the Llano Uplift region. This mixing pattern contrasts with the observed trends in the remaining samples. Notably, the July sampling period depicts a higher  $1/^{88}\text{Sr}$  concentration but intermediate  $^{87}\text{Sr}/^{86}\text{Sr}$  ratios in the lower river area than in December.

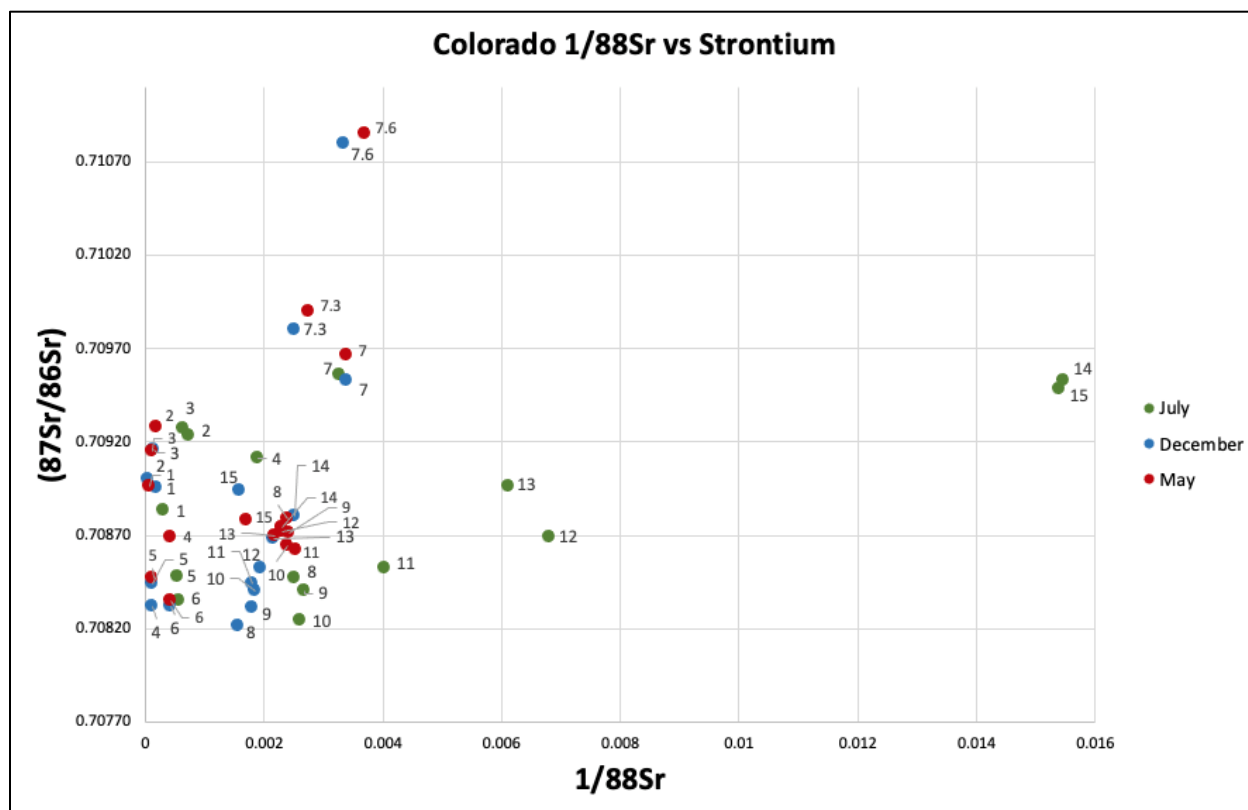


**Figure 26.**  $^{87}\text{Sr}/^{86}\text{Sr}$  ratio vs  $1/^{88}\text{Sr}$  illustrating mixing trends among multiple data points. The relationship between these isotopic ratios provides insights into the mixing processes within the studied system. Points on  $1/^{88}\text{Sr}$  closer to 0 represent a high concentration.

### 3.4. HEAVY METALS

#### 3.4.1 Pecos River

As concentrations of the Pecos River range from 1 to 2.5 ppb. The river's dynamics of Arsenic concentrations vary between seasons, resulting in noticeable differences. In general, rivers in July show much higher concentrations of As than rivers from December, with the exception of PE 3, where the As concentrations are similar in both seasons. In addition, the river shows an increasing trend of As concentrations from upstream to the middle portion of the river (Figure 27). The Maximum Contaminant Level (MCL) for Arsenic in National Primary Drinking Water Regulations (NPDWR), according to the Environmental Protection Agency (EPA), is 0.010 milligrams per liter (mg/L) (“National Primary Drinking Water Regulations | US EPA,” n.d.). The highest value recorded in Pecos is 0.0025 mg/L.

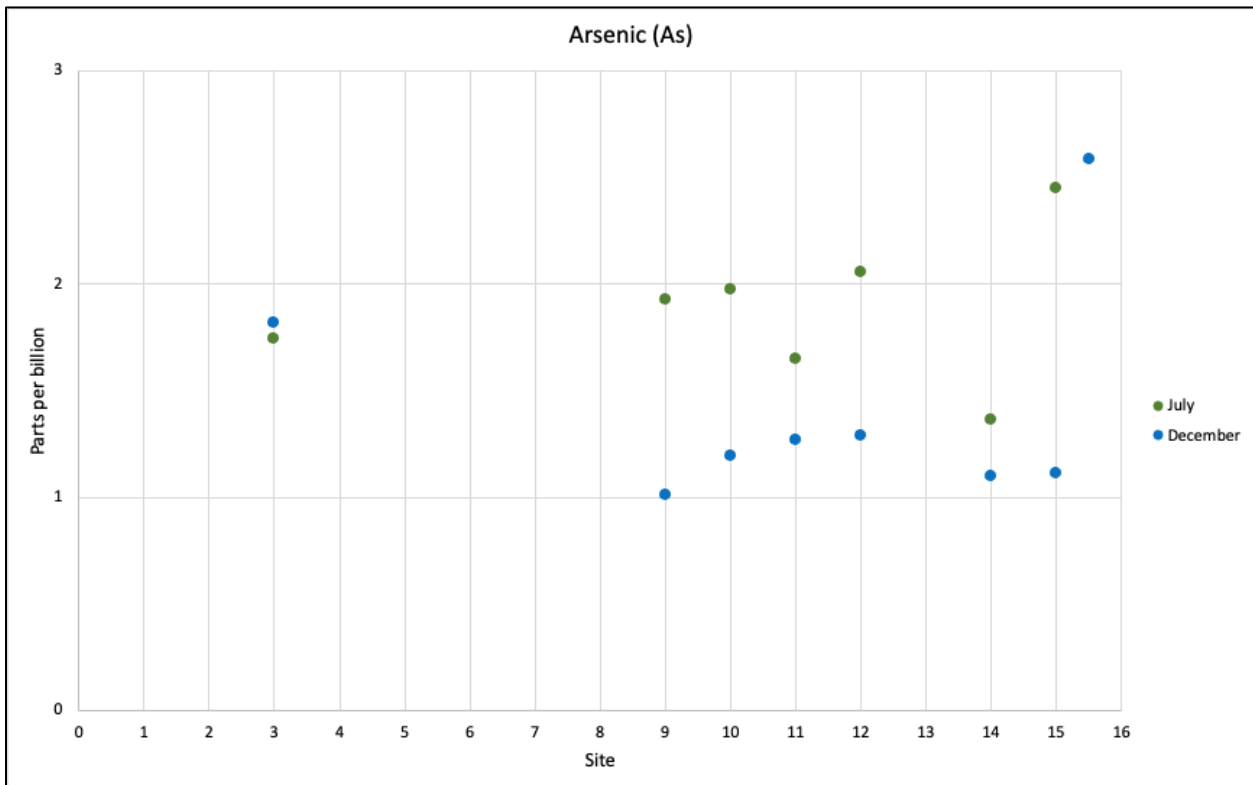


**Figure 27.** Arsenic (As) values in parts per billion (ppb) of the Pecos River.

Lead concentrations exhibit a constant pattern within the upper and middle segments of the river throughout both seasons, most of them below the detection limits of Pb (Figure 28). However, a notable exception arises at site PE 15 during July, where an abnormal value of 70 parts per billion (ppb) is recorded. This value deviates significantly from the previously observed trend. The Maximum Contaminant Level (MCL) for Lead in National Primary Drinking Water Regulations (NPDWR), according to the Environmental Protection Agency (EPA), is 0.015 milligrams per liter (mg/L) (“National Primary Drinking Water Regulations | US EPA,” n.d.). The highest value recorded in Pecos is 0.07 mg/L. The recorded values within the delineated gray box fall below the detection limit.

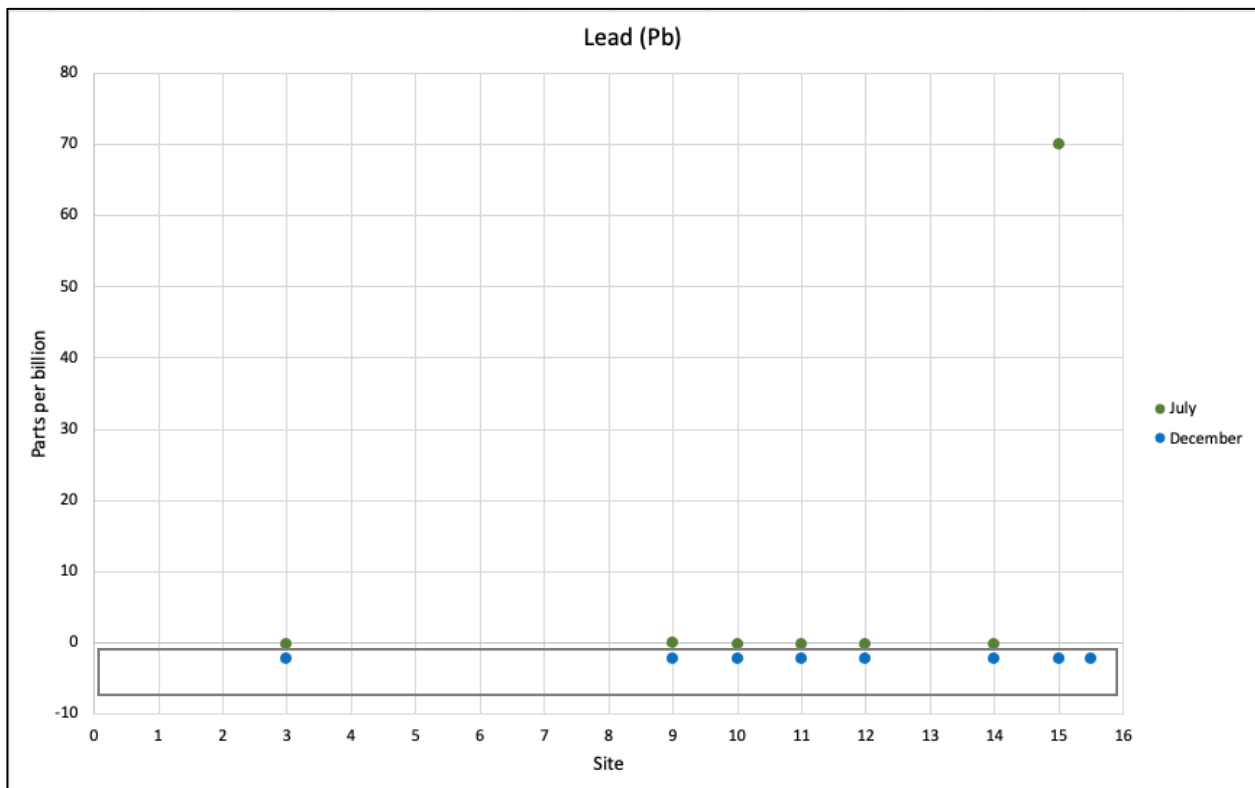


**Figure 28.** Lead (Pb) values in parts per billion (ppb) of the Pecos River.

Boron concentrations in all sites range from 200 to 1800 ppb. The river's dynamics of B concentrations vary between seasons, resulting in noticeable differences. In general, rivers in December show much higher concentrations of B than rivers in July. As the sampling location progresses towards the lowermost part of the river, these values experience a significant decrease. Notably, elevated boron levels are kept at sites PE9 and PE10 within the upper segment of the river. The Maximum Contaminant Level (MCL) for Boron in National Primary Drinking Water Regulations (NPDWR), according to the Environmental Protection Agency (EPA), is 1.4 milligrams per liter (mg/L). The highest value in Pecos is 1.8 mg/L (Epa, 2008).

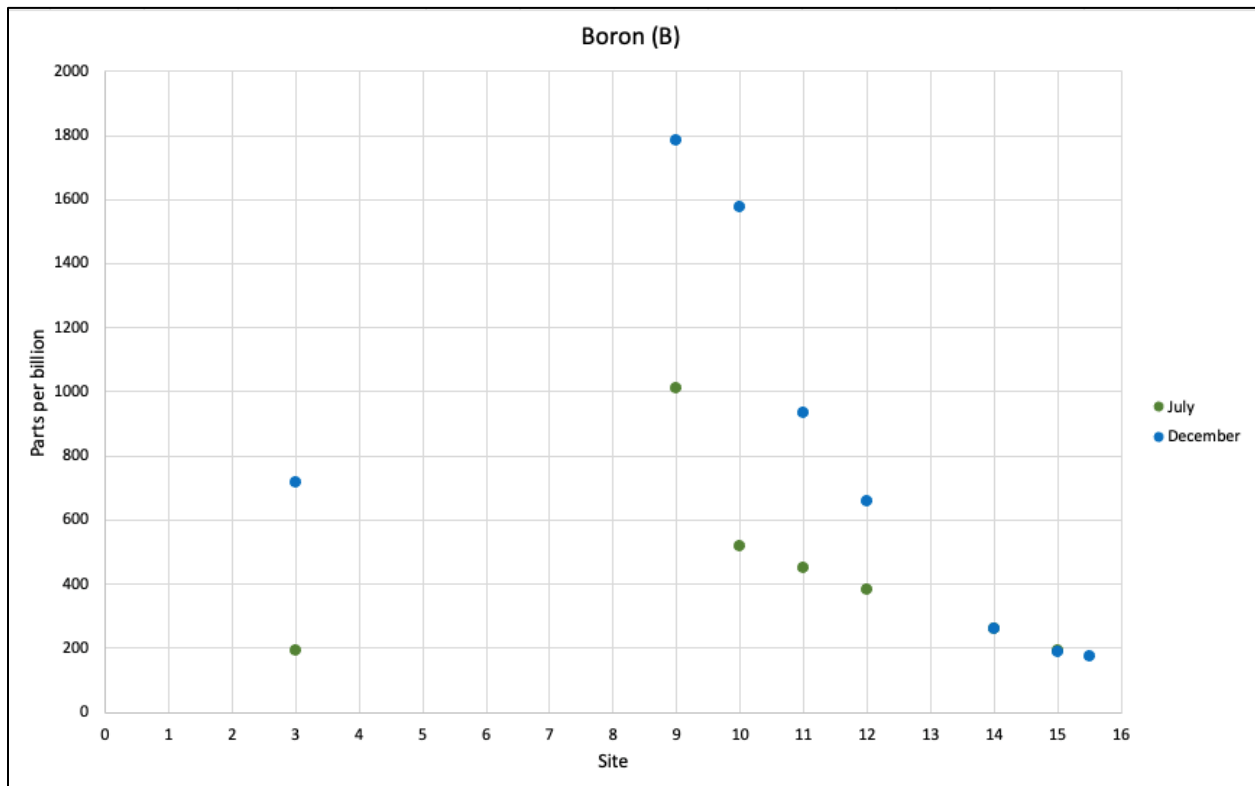


**Figure 29.** Boron (B) values in parts per billion (ppb) of the Pecos River.

Cadmium concentrations in Figure 30 demonstrate a consistent pattern, similar to Pb, during both the months of July and December. However, during July, a significant rise in cadmium levels is observed, specifically at site 15. The Maximum Contaminant Level (MCL) for Cadmium in National Primary Drinking Water Regulations (NPDWR), according to the Environmental Protection Agency (EPA), is 0.005 milligrams per liter (mg/L) (“National Primary Drinking Water Regulations | US EPA,” n.d.). The highest value recorded in Pecos is 0.004 mg/L. The recorded values within the delineated gray box fall below the detection limit.

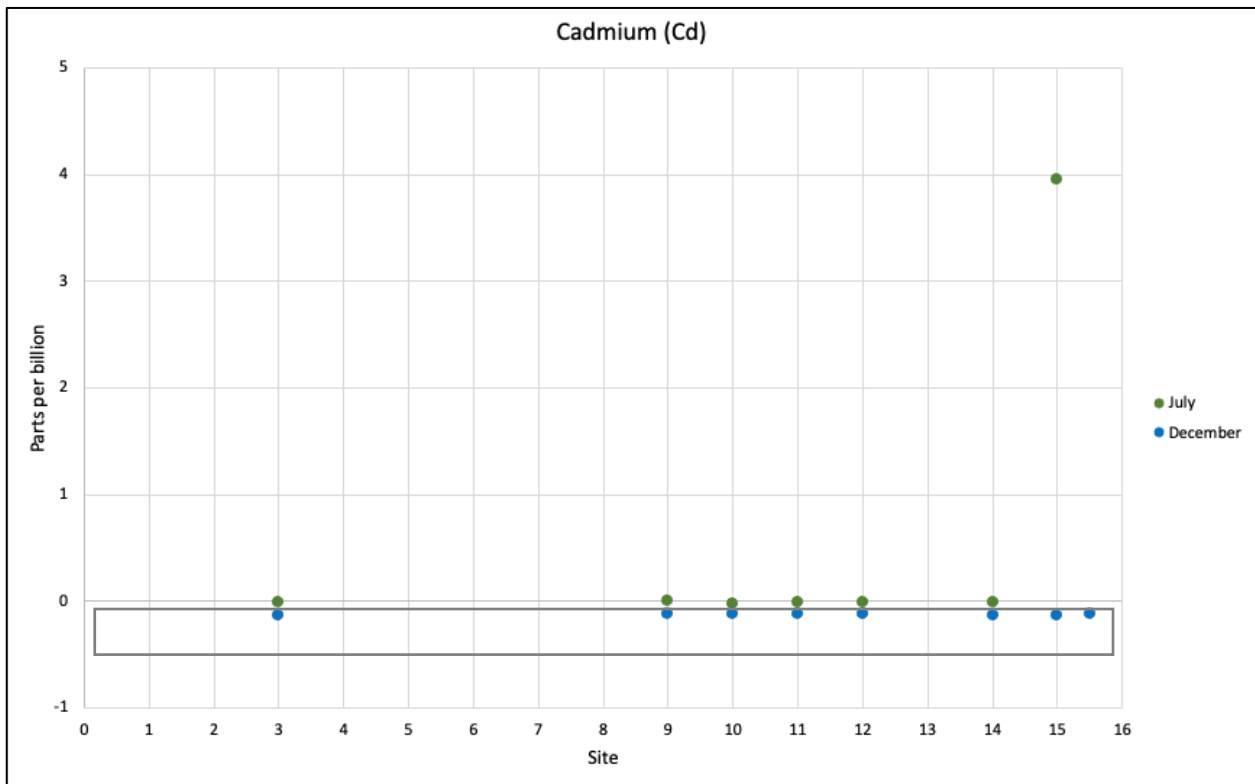


**Figure 30.** Cadmium (Cd) values in parts per billion (ppb) of the Pecos River.



The element vanadium exhibits distinct variations within different regions of the river system and across seasons (Figure 31). In July, site PE 3 in the upper stream area displayed a notable difference in vanadium concentrations compared to other sites. However, concentrations in sites PE 9 and PE 10 appear to be similar. The middle portion of the river (PE 11-PE 15) experiences a significant increase in vanadium levels during both seasons. The pronounced elevation observed at site PE 12 is of particular significance, which stands out among other sampling locations. According to the American Water Works Association, this heavy metal has no federal drinking water standard (“Vanadium,” n.d.).

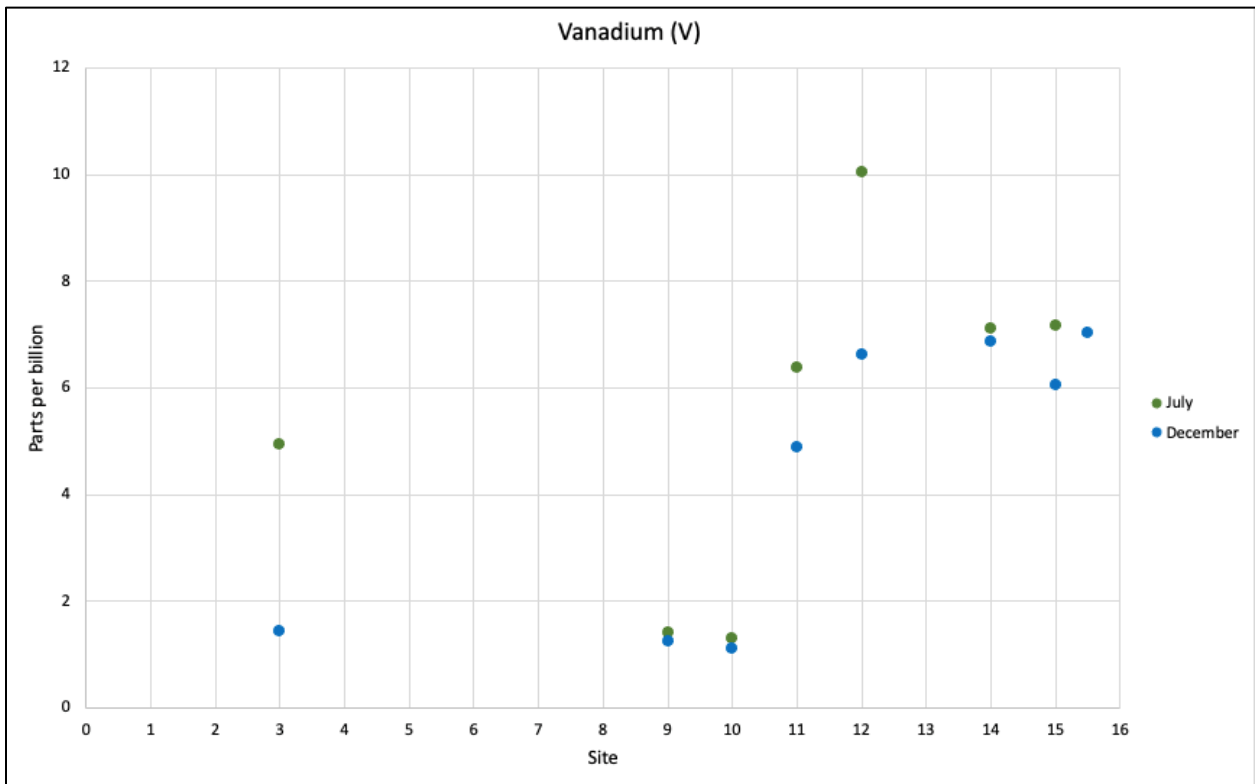


**Figure 31.** Vanadium (V) values in parts per billion (ppb) of the Pecos River.

### ***3.4.2 Colorado River***

Arsenic concentrations of the Colorado river range from 1 to 7 ppb (Figure 32). Samples in July generally show high concentrations compared to the other two sampling seasons (May and December) and exhibit significant variations across multiple sampling sites. For example, Sites CO 1 to CO 4 display a notable and drastic decrease in arsenic values. Subsequently, concentrations also decrease at sites CO 5 to CO 8, followed by an increase and remaining relatively constant values from CO9 to CO 15. In contrast, December CO samples have lower arsenic values. Nevertheless, an upward trend is observed as the sampling reaches the middle and lower portions of the river. Similarly, May samples show a trend comparable to December but with higher peaks at sites CO 2 and CO 4 in the upstream region and sites 14 and 15 in the downstream area. The Maximum Contaminant Level (MCL) for Arsenic in National Primary Drinking Water Regulations (NPDWR), according to the Environmental Protection Agency (EPA), is 0.010 milligrams per liter (mg/L) (“National Primary Drinking Water Regulations | US EPA,” n.d.). The highest value recorded in Colorado is 0.0065 mg/L.

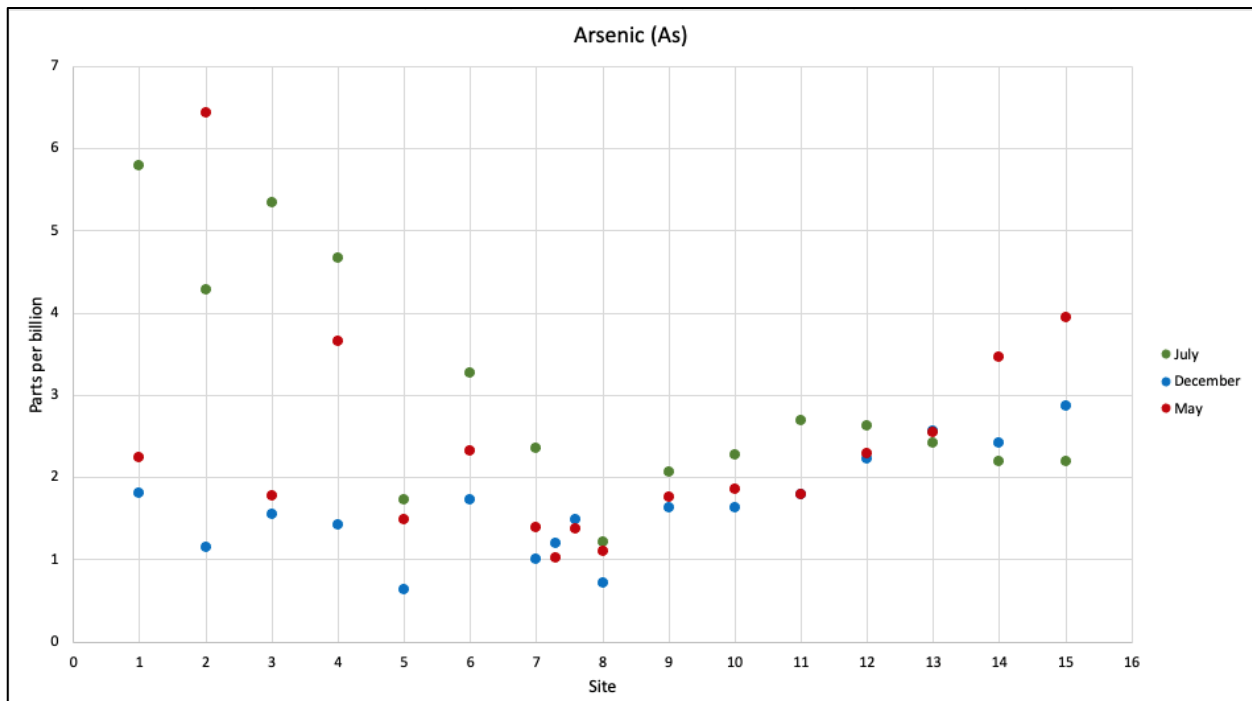


**Figure 32.** Colorado River Arsenic (As) values in parts per billion.

Lead concentrations consistently remain below detection limits across all seasons and exhibit relatively stable patterns. However, there are a few outliers that deviate from the trend. In July, samples show a noticeable difference at site CO 6. During December, specific sites, namely sites CO2, CO 7, CO 7.3, CO 7.6, and CO 9, predominantly located in the middle portion of the river except for site 2 in the upper region, demonstrated higher lead values than the other sampled sites. Lead values observed in May remain consistent across all sampled sites below detection limits. The Maximum Contaminant Level (MCL) for Lead in National Primary Drinking Water Regulations (NPDWR), according to the Environmental Protection Agency (EPA), is 0.015 milligrams per liter (mg/L) (“National Primary Drinking Water Regulations | US EPA,” n.d.). The highest value recorded in Colorado is 0.0165 mg/L. The recorded values within the delineated gray box fall below the detection limit.

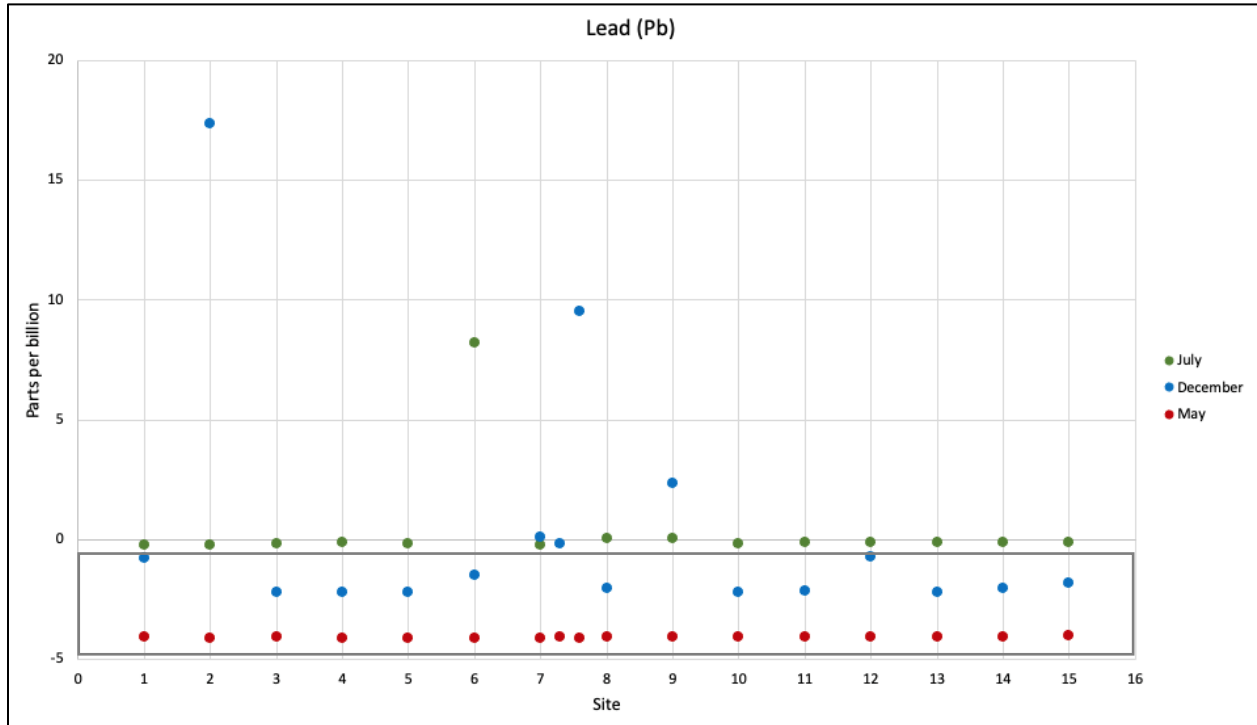


**Figure 33.** Colorado River Lead (Pb) values in parts per billion.

Boron concentrations depicted in Figure 34 exhibit intriguing variations within the upper portion of the river. During July, sites CO 1 to CO 6 demonstrate lower boron values, which subsequently increase during December. Boron values are notably high in May, except for sites CO 2 and 4, which show relatively lower concentrations. An important observation is a drastic decrease in boron concentrations as the river transitions into the middle and lower portions. These concentrations remain consistently low throughout these river sections. The Maximum Contaminant Level (MCL) for Boron in National Primary Drinking Water Regulations (NPDWR), according to the Environmental Protection Agency (EPA), is 1.4 milligrams per liter (mg/L). The highest value recorded in Colorado is 2.6 mg/L (Epa, 2008).

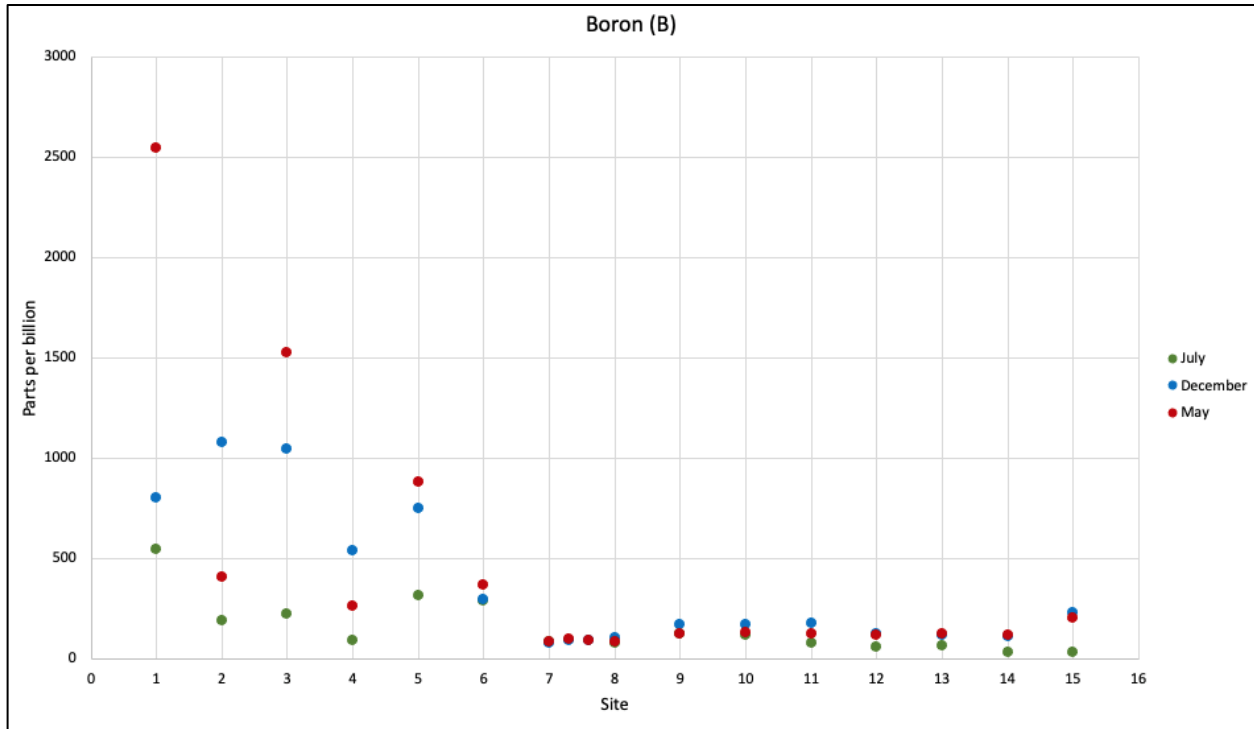


**Figure 34.** Colorado River Boron (B) values in parts per billion.

Cadmium samples consistently remain below detection limits and exhibit relatively stable patterns across all seasons. However, there are a few outliers that deviate from the trend. In July, samples show a noticeable difference in site CO 6. In December, specific sites, namely sites CO2, CO 7, CO 7.3, 7.6, and CO9 predominately located in the middle portion of the river show an increase except for site 2 in the upper region, demonstrating a higher cadmium value than the other sample sites. May levels remain lower compared to the other two months. The Maximum Contaminant Level (MCL) for Cadmium in National Primary Drinking Water Regulations (NPDWR), according to the Environmental Protection Agency (EPA), is 0.005 milligrams per liter (mg/L) (“National Primary Drinking Water Regulations | US EPA,” n.d.). The highest value recorded in Colorado is 0.000298 mg/L. The recorded values within the delineated gray box fall below the detection limit.

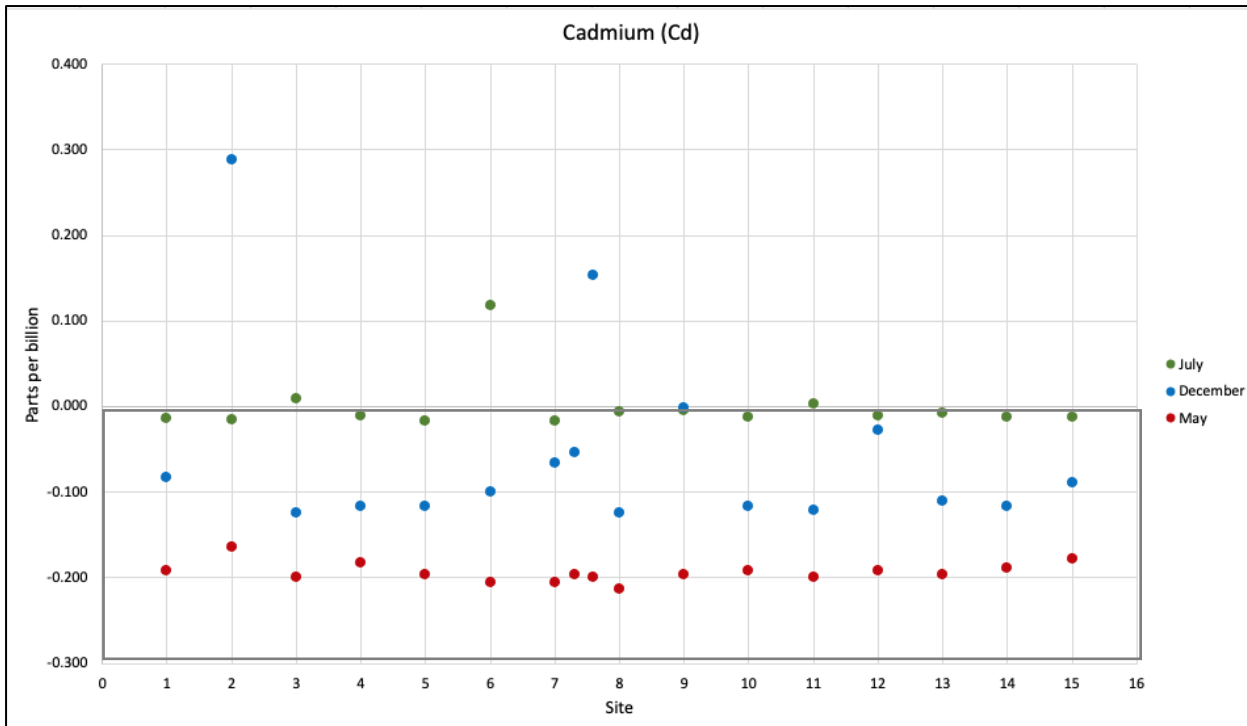


**Figure 35.** Colorado River Cadmium (Cd) values in parts per billion.

In July, the upper region of the river exhibited higher values of vanadium, which subsequently experienced a significant decrease (Figure 36). This decreasing trend follows a pattern like in the December samples from the middle and lower regions of the river. Notably, December samples generally maintain lower values, except for site CO 1. Furthermore, May samples CO sites 2 and 3 display notably high values, which then decrease drastically. The middle to lower regions of the river demonstrates an increasing trend as the sampling locations approach the river's lower portion. According to the American Water Works Association, there is no federal drinking water standard for this heavy metal (“Vanadium,” n.d.).

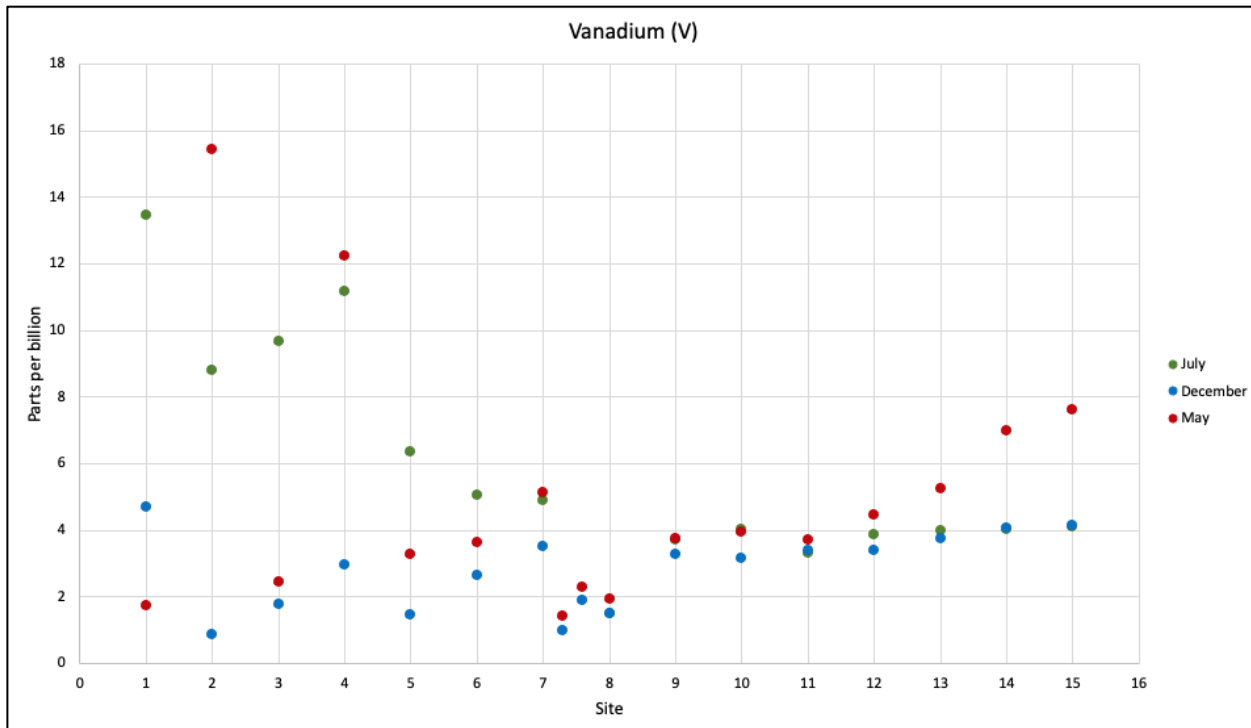


**Figure 36.** Colorado River Vanadium (V) values in parts per billion.

#### 3.4.4 T-TEST

A student's t-test was performed to understand if means of subsample groups are different from each other between seasons. This was conducted for  $87\text{Sr}/86\text{Sr}$ ,  $\delta^{18}\text{O}$  and  $\delta\text{D}$  ratios on different seasons for Pecos and Colorado rivers. A paired two-samples-per-mean calculation was used to create this test with an alpha of 0.05 (significance level). In addition, a two-tailed hypothesis was selected to understand if there is a significant difference between samples on different seasons (May, July, December) or not.

Table 2. Student's T-test paired two samples of means.

<b>Two Samples of Means</b>	<b>Significant or Non-significant</b>	<b>T-Statistic</b>
Pecos $\delta^{18}\text{O}$ July vs. December	Significant	-0.601347
Pecos $\delta\text{D}$ July vs. December	Not significant	-0.3221
Pecos 87/86Sr July vs. December	Not significant	0.165333
Colorado $\delta^{18}\text{O}$ July vs. December	Not significant	-1.787873
Colorado $\delta\text{D}$ July vs. December	Not significant	-1.220544
Colorado 87/86Sr July vs. December	Significant	2.848098
Colorado $\delta^{18}\text{O}$ December vs. May	Significant	-2.658236
Colorado $\delta\text{D}$ December vs. May	Significant	-2.827537
Colorado 87/86Sr December vs. May	Significant	-2.903012
Colorado $\delta^{18}\text{O}$ July vs. May	Significant	4.002977
Colorado $\delta\text{D}$ July vs. May	Significant	4.064619
Colorado 87/86Sr July vs. May	Significant	-0.633124

Eight relationships were statistically significant based on the t-test analysis, with their meaningful associations. Contrariwise, four relationships yielded non-significant results, suggesting a lack of statistically meaningful connections in these relationships.



### 3.4.5 IMPLICATIONS FOR SOCIETY AND ECOSYSTEMS

The outcomes of this study hold significance for the public, highlighting the vital understanding of how water quality fluctuates across diverse river sites throughout the state. Water quality increases close to coastal regions, and salinity levels diminish as we move to the coast. This study carries profound implications that can produce awareness among water management industries and policymakers, prompting them to prioritize the well-being of their citizens. Specifically, the investigation of the Pecos River reveals salinity concerns in its water sources, confirming the underlying causes. Both rivers are essential resources for agriculture, leisure, and urban activities, so their health is essential. The ecosystem's complex balance, surrounding many plant and animal species, is tied to river health. Alterations in water composition or chemical substances (e.g., heavy metals) can disturb the functioning equilibrium of this ecosystem. Recognizing our interconnectedness within this expansive ecosystem highlights the importance of collective study and preservation. Moreover, it is significant that the worsening of water scarcity, a consequence of climate change, could intensify the challenges in regions struggling with limited water availability.

## CHAPTER 4: DISCUSSION

### 4.1 WATER STABLE ISOTOPES: WHERE IS THE WATER COMING FROM DIFFERENT PORTIONS OF THE WATERSHED?

As discussed in the conceptual model of watershed boundaries presented by Condon et al. (Figure 4), the hydrological dynamics within a watershed involve rainwater infiltration into the soil, predominantly occurring during the summer (monsoon) and subsurface flow paths from shallow and deep aquifers. To comprehensively understand the structure of a watershed and the pathways of water movement within it, multiple factors must be considered. Among these factors is groundwater recharge, which involves replenishing subsurface water resources that flow considerable distances before recharging into the river system, known as groundwater discharge or baseflow. Furthermore, it is essential to acknowledge the potential presence of deep groundwater zones that may display brine upwelling, denoting the upward migration of highly saline solutions toward the surface. Brine upwelling can be observed in the hydrocarbon-rich Wolfcamp formation, known for its oil and gas reservoirs. It is mainly located in the upper regions of the Pecos and Colorado sample study sites. Consequently, the watershed under investigation may exhibit mixing patterns from diverse water sources with surface, shallow and deep flow paths. The analysis presented in Figure 6 focuses on the meteoric relationship between stable isotope ratios of  $^{18}\text{O}$  and  $^2\text{H}$  in our water samples. This approach enables the examination of the isotopic signature of water molecules, providing insights into their origin and source. Using the Global Meteoric Water Line (GMWL) as a reference, we can interpret the positioning of our samples to this line. Samples in the plot's upper right display higher isotope ratios, indicating a heavier composition typically associated with the summer season. On the other hand, samples in the lower left display lower isotope ratios, suggesting a more depleted composition commonly observed

during winter. It is important to note that the specific location of samples on the plot may vary depending on the geographic location. Generally, water tends to be heavier in coastal areas and progressively lighter as one moves away from the coast. Using this plot, we aim to understand our results and their implications.

The upper portion of the Colorado River (Figure 27, A) exhibits distinct isotopic patterns and variations. In July, the presence of rainwater inflow and precipitation is evident, as indicated by the isotopic values of the samples. However, evaporation processes show a noticeable increase from December to May, leading to higher isotopic values and a shift toward baseflow contributions. This is further supported by brine signatures in samples 1, 2, and 6, indicating potential influences from subsurface brine sources. Another contributing factor to the observed isotopic variations in May and December could be the prolonged residence time of the samples in the river, allowing for increased evaporation effects. Our investigation of the upper section of the Pecos River (Figure 27, B) also reveals the contribution of brines originating from the Wolfcamp formation. This is observed in samples 3, 9, and 10 in Pecos River during both seasons, indicating a consistent brine contribution. Moreover, sample 3, located close to the Global Meteoric Water Line (GMWL), can be attributed to the impact of precipitation during the monsoon and less brine contribution. According to the conceptual diagram presented by Dutton et al. (Figure 28), there is a proposed mixing scenario involving sedimentary brines derived from the Wolfcamp formation. These brines are believed to interact with the underlying freshwater system and gradually make their way to the Pecos River as well as Colorado river in this region. This conceptual model explains the presence of brines observed in the Pecos area, indicating a potential influence of subsurface brine sources on the river water composition.

Unlike the upper section of the Colorado River, samples 7 to 11 in Colorado exhibit the absence of brine contributions originating from the upper region. Instead, this section corresponds to a carbonate aquifer system, including the Carrizo-Wilcox, Edwards, and Trinity aquifers, as mentioned in Figure 11. Notably, many samples align with the location of the carbonate aquifer region, as illustrated in Figure 27C. This emphasizes the significant influence of the underlying carbonate formations on the isotopic composition of the water samples. Moreover, the increased frequency of rainfall events in this area becomes evident, as indicated by the closer proximity of the samples to the Global Meteoric Water Line (GMWL). Important patterns can be observed in the data: while the samples collected in July and December exhibit a downward shift along the GMWL, the May samples display an upward trend, resembling an evaporation trend moving from the reference line.

The middle section of the Pecos River is characterized by the Edwards aquifer, a carbonate-based aquifer system, as mentioned in Figure 11. Therefore, this region's distinctive brine signatures observed in previous sections are absent. Instead, our analysis reveals that the water samples collected in July and December exhibit closer proximity to the aquifer area and align more closely with the Global Meteoric Water Line (GMWL), as illustrated in Figure 27D. This indicates a more substantial influence from the Edwards aquifer and suggests a greater connection to the regional hydrological system. Additionally, the middle portion of the Pecos River experiences increased precipitation.

The downstream section of the Colorado River corresponds to a silicate aquifer or Gulf Coast aquifer, as illustrated in Figure 11. In this region, the water-stable isotopes consistently align above the Global Meteoric Water Line (GMWL). This observation can be attributed to the continuous water cycle and regular precipitation during the summer and winter seasons, as mentioned in

Figure 27E. Notably, the May samples display a distinct separation from the GMWL. This separation from the expected trend could indicate an evaporation process or the influence of water signatures originating from upstream and middle stream regions. It is possible that these upstream and middle stream water sources contribute to the river's water composition during periods of reduced precipitation. An alternative explanation for the distinct isotopic signatures observed in the carbonate and silicate aquifers during the dry season (May) is the potential influence of brine water flow originating from upstream areas. This brine water may flow through the middle stream and ultimately reach the lower portion of the river during periods of low to no rainfall. The interconnected nature of the river system allows for the possibility of such brine water transport, thereby contributing to the observed variations in isotopic compositions.

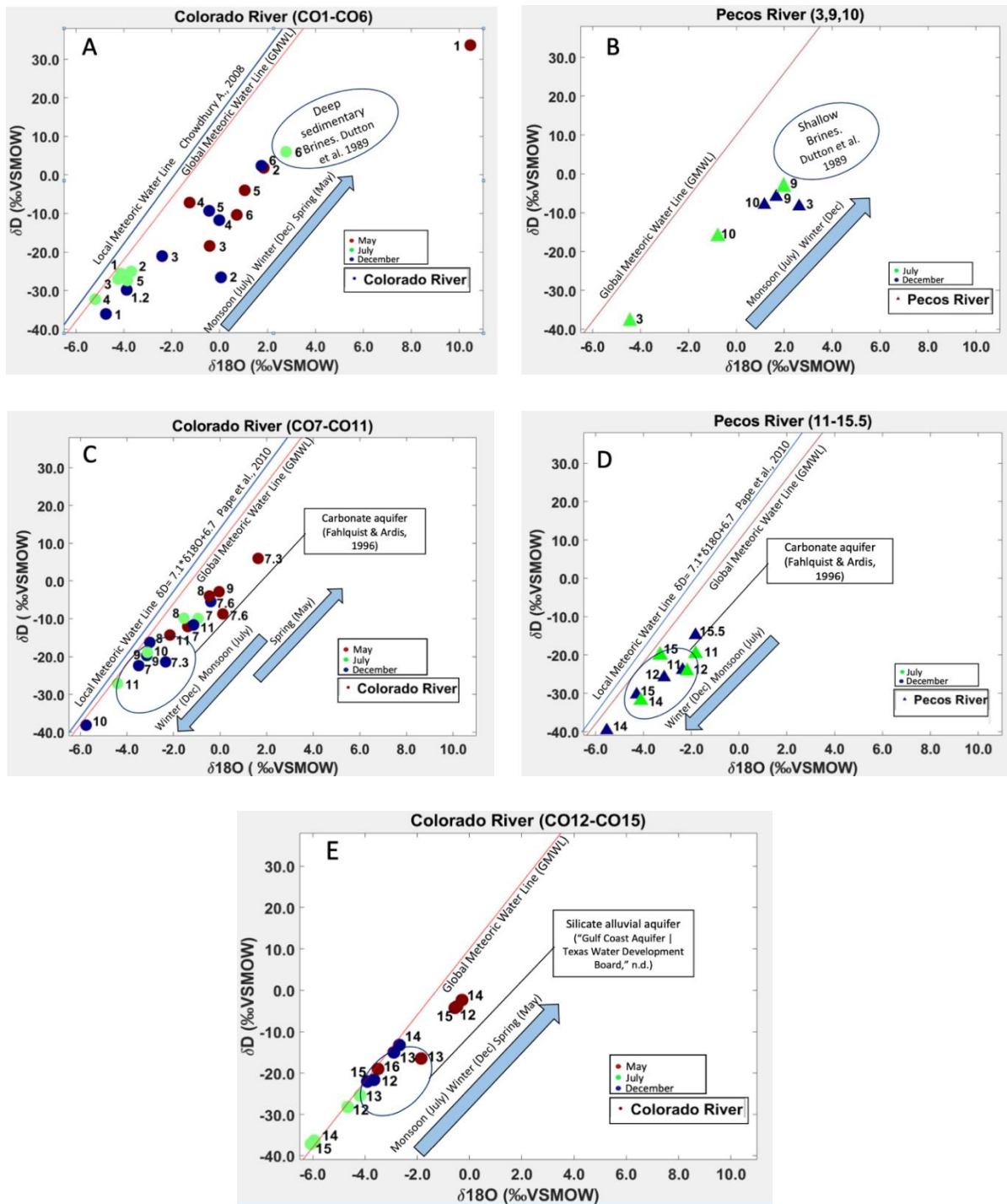


**Figure 37.**  $\delta^2\text{H}$  and  $\delta^{18}\text{O}$  (‰VSMOW) plots portraying the distribution of all samples divided into three sections: upper, middle, and lower. The upper portion of the Colorado River with samples 1 to 6 (A). The upper portion of the Pecos River with samples 3, 9, and 10 (B). The middle portion of the Colorado River with samples 7 to 11 (C). The middle portion of the Pecos River with samples 11 to 15.5 (D). The lower portion of the Colorado River with samples 12 to 15 (E). The Global Meteoric Water Line (GMWL) is a standard value  $\delta^2\text{H} = 8 * \delta^{18}\text{O} + 10\text{‰ SMOW}$ .

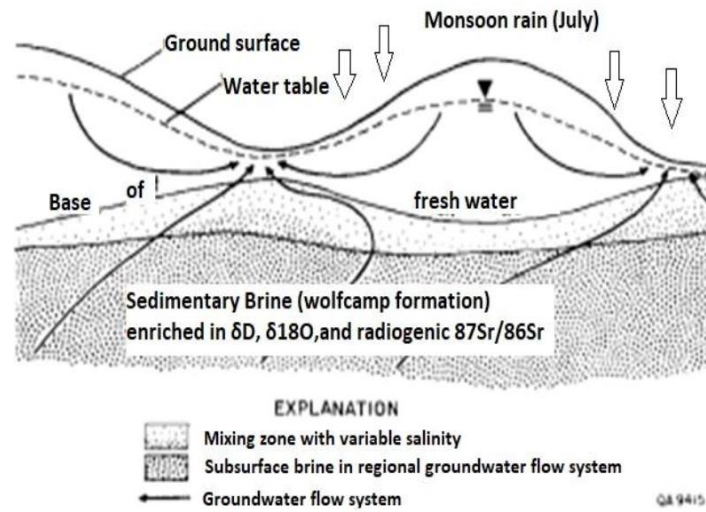


**Figure 38.** The sedimentary brines conceptual model of groundwater mixing was modified from Dutton et al., 1989.

The Pecos River's electrical conductivity (EC) exhibits variations between its upper and middle portions. As depicted in Figure 19, samples from the upper area (3, 9, 10) display EC values ranging from 10,000  $\mu\text{s}/\text{cm}$  to 30,000  $\mu\text{s}/\text{cm}$ , indicating a brine-dominated environment. Moving towards the middle carbonate section of the river (samples 11-15.5), EC values decreased from 10,000  $\mu\text{s}/\text{cm}$  to 999  $\mu\text{s}/\text{cm}$  as the river approached the Rio Grande. This reduction can be attributed to increased precipitation and the carbonate aquifer, a salt-diluting agent. A similar trend is observed in the Colorado River (Figure 20), where the upper region exhibits EC values ranging from 1,500  $\mu\text{s}/\text{cm}$  to 45,000  $\mu\text{s}/\text{cm}$ , indicating a brine-dominated area. In the middle portion, the EC decreases from 800  $\mu\text{s}/\text{cm}$  to 400  $\mu\text{s}/\text{cm}$ , reflecting a higher degree of water dilution in the carbonate aquifer compared to the upper portion. Lastly, the lower section of the Colorado River shows EC values ranging from 2,000  $\mu\text{s}/\text{cm}$  to 100  $\mu\text{s}/\text{cm}$ . Some samples overlap between different seasons, but the lower section consistently exhibits EC values within this range during both July

and December sampling periods. The upper reaches of both rivers exhibit elevated salinity levels, which may be influenced by brines.

#### 4.2 STRONTIUM ISOTOPES RATIO

The  $^{87}\text{Sr}/^{86}\text{Sr}$  ratio is a valuable tool for comprehending water resources as it provides insights into the geological materials, including minerals and rocks, that exist within a particular area. When dissolved or weathered, these geological materials become diluted and transported by water. Therefore, we can learn about its potential origin by examining the strontium isotopic composition within the water. Figure 7, a conceptual model, outlines the assigned strontium values across the United States, which will serve as a guiding framework for our research in discerning the source of the water. As previously indicated in Figure 7, it is expected that both the Pecos and Colorado rivers will have strontium values falling within the range of 0.707 and 0.720. The Llano Uplift region was anticipated to range from 0.750 to 0.816. Figure 21 illustrates that the strontium values observed for the Pecos River fall within the range of 0.7075 to 0.7085.  $^{87}\text{Sr}/^{86}\text{Sr}$  does not vary as much between samples but within the  $\delta^{18}\text{O}$  values. In contrast, Figure 22 shows that the Colorado River values are between 0.7080 to 0.7110. Pecos and Colorado rivers have a similar range for  $\delta^{18}\text{O}$  values but a higher variation in  $^{87}\text{Sr}/^{86}\text{Sr}$  for Colorado. Both rivers' strontium values align with the expected outcomes from the conceptual model. Furthermore, the Llano Uplift region results range from 0.7098 to 0.71085. It is essential to mention that strontium values change with different lithology and pick up values from this. The relatively high  $^{87}\text{Sr}/^{86}\text{Sr}$  ratios in upper Colorado river regions are consistent with the notion of upwelling deep basin brines that have a more radiogenic signature compared to evaporite lithology that is present at shallow aquifers in this region. Indeed, the upper Pecos River is dominated by less radiogenic Sr isotope signatures,



most likely due to less upwelling of deep brines compared to the upper Colorado region. Similarly, as in the water-stable isotopes, it is believed the upper region of Pecos and Colorado has a high salinity level due to the brines in this region, but from shallow vs. deep sources. We believe that water flows through the river during the rainy season until it reaches the carbon aquifer.

The Pecos River's  $1/EC$  exhibits variations between its upper and middle portions. Figure 23 describes samples from the upper area (3, 9, 10) display proximity to zero (very high EC values), indicating a brine-dominated environment. However, the highest value corresponds to PE 3 in December. Moving towards the middle carbonate section of the river (samples 11-15.5),  $1/EC$  values decreased to a closer value of  $0.001 \mu\text{s}/\text{cm}$  as the river approached the Rio Grande. This reduction can be attributed to increased precipitation and the carbonate aquifer, a salt-diluting agent. A similar trend is observed in the Colorado River (Figure 24), where the upper region exhibits higher  $1/EC$  values ( $0$  to  $0.001 \mu\text{s}/\text{cm}$ ) in a brine-dominated area. In the middle portion, the  $1/EC$  decreases but has a higher  $^{87}\text{Sr}/^{86}\text{Sr}$  of  $0.7085$  and  $0.7011$  in the carbonate aquifer. Here we have a lower electrical conductivity due to the increased dilution in the area. Lastly, the lower section of the Colorado River shows  $1/EC$  values ranging from  $0.0015$  to over  $0.005 \mu\text{s}/\text{cm}$ . Samples CO 14 and CO 15 are the ones at the coast that have the least electrical conductivity. Multiple samples overlap between different seasons, but the upper reaches of both rivers exhibit elevated salinity levels, which may be influenced by brines. Figures 25 (Pecos) and 26 (Colorado), representing the  $^{87}/^{86}\text{Sr}$  vs.  $^{1}/^{88}\text{Sr}$  isotopic ratio, are very similar to the  $1/EC$  plots previously discussed.

### 4.3 TRACE METALS

Trace metals are naturally present in water bodies and hold significant environmental importance, typically quantified in parts per billion (ppb). However, land use practices can notably influence the abundance of these trace metals in water. As mentioned in Figure 5, human activities can introduce additional contaminants. Various land use activities, such as agriculture, industrial processes, mining, and residential development, among others, play roles in shaping the concentrations in water. Figures 27 (PE) and 32 (CO) show higher concentrations of Arsenic in water during July. Additionally, Figure 32 (CO) reveals variations in Arsenic levels in May. The data displays fluctuations in Arsenic concentrations across different sampling sites, with CO 2 (Scurry County), 4 (Coke County), and 6 (Coleman and Mcculloch County) exhibiting significantly elevated values compared to adjacent sites. Arsenic can be present in mining activities, agriculture (pesticides or fertilizers), and even on certain rocks and minerals. It is important to mention, Arsenic is observed to be higher in the upper region of Colorado and the lower portion of Pecos, most likely due to the upwelling of basin brines in this region.

Lead concentrations, Figure 28 (PE) only peak in July, with site 15 (Val Verde County) concentration of 70 ppb, whereas the other samples indicate lower and relatively stable levels. In Figure 33 (CO), Lead levels demonstrate peaks in December at samples 2 (Scurry County), 7.6 (Burnet County), and 9 (Bastrop County) and in July at site 6 (Coleman and Mcculloch County), with 16 to 3 ppb concentrations. Lead can be found in landfills, water, and even industry discharges. Similarly, Cadmium levels in December (CO) indicate increased samples 2 (Scurry County) and 7.6 (Burnet County) and higher concentrations at site 6 (Coleman and Mcculloch counties) in July. Cadmium can be found in mining activities, industrial discharge, and present in pipe corrosion.

Higher Boron values in Figure 29 (PE) can be found in the lower portion of the river in Pecos, Crockett, Terrel, and Val Verde counties during the month of December. Its values range from 1800 to 620 ppb, followed by a gradual decrease in concentration. In Colorado (Figure 24), Boron concentrations in May depict higher values in sample 1 (Borden County), exhibiting a gradual decline through sample 6 (upper) (Coleman and McCulloch), with concentrations ranging from 2500 to 400 ppb. Boron can be naturally found in rocks and minerals, but anthropically can be found in fertilizers and industrial waste. As for Cadmium concentrations, Figure 30 (PE) displays a higher value in July for the lower region, notably at sample 15, which records four ppb in Val Verde County in Colorado (Figure 35).

Lastly, Vanadium concentrations in Figure 31 (PE) reveal elevated values ranging from 4.5 to 6.5 ppb in July and December, particularly notable in samples 3 (Pecos County), 11 (Pecos and Crockett County), 12 (Terrel and Crockett County), and 14 (Val Verde County). However, sample 3 in December exhibits a lower value. In contrast, Figure 36 (CO) illustrates high Vanadium values only in May, specifically in samples 2 (Scurry County) and 3 (Mitchell County), while July exhibits elevated values in samples from the upper region of the river. Furthermore, Vanadium concentrations demonstrate a drastic decline in the middle portion and begin to increase again in the river's lower portion. Vanadium is known to be found in water due to industrial, mining, discharge, landfills, and even in the oil industry. Most peaks in heavy metals observed have been present during the month of July for both rivers. In addition to some in May, few peaks are observed in December. This might point out that extra activity may be present during the month of July that can change the chemistry of the rivers. Arsenic and Boron are associated with shallow and deep brines, possibly indicating their presence from geological formations rich in brine content. Lead and Cadmium are likely attributable to industrial activities, which release into the

water from anthropogenic sources. Lastly, Vanadium's association with deep brines is likely influenced by oil contributions.

## CHAPTER 5: CONCLUSION

In conclusion, the findings of this study reveal stable and highly brine upwelling in the upper reaches of the Pecos and Colorado Rivers. This can be attributed to the Wolfcamp Formation, known for its oil and gas reservoirs. As a result, the investigated watershed exhibits the likelihood of mixing patterns originating from diverse water sources, including surface, shallow, and deep flow paths. The assumption of such mixing patterns is further supported by the area's observed high electrical conductivity values. In the middle reaches of the Colorado River, there is a notable absence of brine contributions due to a carbonate aquifer with higher levels of rainfall. Consequently, water dilution is observed, evident in the reduction of electrical conductivity values in this region. Similarly, the middle portion of the Pecos River also exhibits a lower presence of brines, as corroborated by the comparatively lower electrical conductivity values. The lower reaches of the Colorado River, particularly during May, show indications of possible evaporation due to reduced precipitation during that season. Additionally, the contributions of water from upper and middle stream sources to the river's water composition during reduced precipitation are also noticeable, as explained by some May samples showing higher electrical conductivity values in the lower portion.

An alternative explanation for the distinct isotopic signatures observed in the carbonate and silicate aquifers during the dry season (May) is the potential influence of brine water flow originating from upstream areas. This brine water may travel through the middle stream and ultimately reach the lower portion of the river during periods of low to no rainfall.

Naturally occurring elements,  $^{87}\text{Sr}/^{86}\text{Sr}$ , and heavy metals are influenced by various processes and factors, including anthropogenic, geological, and chemical. The upwelling brines in the upper Pecos and Colorado rivers contribute to higher Strontium values and Arsenic concentrations, with both elements associated with shallow and deep brines in the region. Vanadium is also present in the Pecos and lower Colorado regions, mainly from deep brines with oil contributions. The middle portion of the Colorado River exhibits elevated levels of lead and

cadmium, commonly associated with industrial activities. The Llano uplift is known for being very high for  $^{87}\text{Sr}/^{86}\text{Sr}$ . Furthermore, the lower portion of the Colorado River shows increased Vanadium presence, potentially sourced from deep brines. Strontium also exhibits a moderate average in this region. Like water-stable isotopes, it is plausible that brines are transported and integrated into the river flow as it moves downstream from upstream sources.

## REFERENCES

- Barbieri, M., Boschetti, T., Petitta, M., & Tallini, M. (2005). Stable isotope ( $^2\text{H}$ ,  $^{18}\text{O}$  and  $^{87}\text{Sr}/^{86}\text{Sr}$ ) and hydrochemistry monitoring for groundwater hydrodynamics analysis in a karst aquifer (Gran Sasso, Central Italy). *Applied Geochemistry*, 20(11), 2063–2081.  
<https://doi.org/10.1016/j.apgeochem.2005.07.008>
- Bataille, C. P., & Bowen, G. J. (2012). Mapping  $^{87}\text{Sr}/^{86}\text{Sr}$  variations in bedrock and water for large scale provenance studies. *Chemical Geology*, 304–305, 39–52.  
<https://doi.org/10.1016/j.chemgeo.2012.01.028>
- BEG Maps of Texas - Geology - LibGuides at University of Texas at Austin. (n.d.). Retrieved July 31, 2022, from <https://guides.lib.utexas.edu/geo/beg-maps>
- Carrizo-Wilcox Aquifer | Texas Water Development Board. (n.d.). Retrieved July 31, 2022, from <https://www.twdb.texas.gov/groundwater/aquifer/majors/carrizo-wilcox.asp>
- Chihuahuan Desert Ecoregion (U.S. National Park Service). (n.d.). Retrieved July 17, 2022, from <https://www.nps.gov/im/chdn/ecoregion.htm>
- Clark, I. D. (Ian D., & Fritz, P. (Peter). (1997). *Environmental isotopes in hydrogeology*. CRC Press/Lewis Publishers.
- ColoradoRiverBasinPoster. (n.d.).
- Condon, L. E., Markovich, K. H., Kelleher, C. A., McDonnell, J. J., Ferguson, G., & McIntosh, J. C. (2020). Where Is the Bottom of a Watershed? *Water Resources Research*, 56(3), e2019WR026010. <https://doi.org/10.1029/2019WR026010>
- Crowley, B. E., Miller, J. H., & Bataille, C. P. (2017). Strontium isotopes ( $^{87}\text{Sr}/^{86}\text{Sr}$ ) in terrestrial ecological and palaeoecological research: empirical efforts and recent advances in continental-scale models. *Biological Reviews*, 92(1), 43–59.  
<https://doi.org/10.1111/brv.12217>
- Dutton, A. R., Richter, B. C., & Kreitler, C. W. (1989). Brine Discharge and Salinization, Concho River Watershed, West Texas. *Groundwater*, 27(3), 375–383.  
<https://doi.org/10.1111/j.1745-6584.1989.tb00461.x>
- Edwards (Balcones Fault Zone) Aquifer | Texas Water Development Board. (n.d.). Retrieved July 31, 2022, from <https://www.twdb.texas.gov/groundwater/aquifer/majors/edwards-bfz.asp>
- Edwards-Trinity (Plateau) Aquifer | Texas Water Development Board. (n.d.-a). Retrieved July 26, 2022, from <https://www.twdb.texas.gov/groundwater/aquifer/majors/edwards-trinity-plateau.asp>
- Edwards-Trinity (Plateau) Aquifer | Texas Water Development Board. (n.d.-b). Retrieved July 31, 2022, from <https://www.twdb.texas.gov/groundwater/aquifer/majors/edwards-trinity-plateau.asp>
- Eley, B. (n.d.). *Causes of Depletion of the Pecos River in New Mexico AP A 2 105 3 UNIVERSITY OF CALIFORNIA*.
- Epa, U. (2008). *EPA-OGWDW Regulatory Determinations Support Document for CCL 2 Regulatory Determinations Support Document for Selected Contaminants from the Second Drinking Water Contaminant Candidate List (CCL 2) Part II: CCL 2 Contaminants Undergoing Regulatory Determination*.
- File:Texas population map.png - Wikimedia Commons. (n.d.). Retrieved September 17, 2022, from [https://commons.wikimedia.org/wiki/File:Texas\\_population\\_map.png](https://commons.wikimedia.org/wiki/File:Texas_population_map.png)

- Garcia, S., Louvat, P., Gaillardet, J., Nyachoti, S., & Ma, L. (2021). Combining Uranium, Boron, and Strontium Isotope Ratios ( $^{234}\text{U}/^{238}\text{U}$ ,  $\delta^{11}\text{B}$ ,  $^{87}\text{Sr}/^{86}\text{Sr}$ ) to Trace and Quantify Salinity Contributions to Rio Grande River in Southwestern United States. *Frontiers in Water*, 2. <https://doi.org/10.3389/frwa.2020.575216>
- Geology of Texas | TX Almanac. (n.d.). Retrieved September 17, 2022, from <https://www.texasalmanac.com/articles/geology-of-texas>
- Gregory, L. (n.d.). A Watershed Protection Plan for the Pecos River in Texas.
- Gulf Coast Aquifer | Texas Water Development Board. (n.d.). Retrieved July 31, 2022, from <https://www.twdb.texas.gov/groundwater/aquifer/majors/gulf-coast.asp>
- Li, X., Weng, B., Yan, D., Qin, T., Wang, K., Bi, W., et al. (2019). Anthropogenic effects on hydrogen and oxygen isotopes of river water in cities. *International Journal of Environmental Research and Public Health*, 16(22). <https://doi.org/10.3390/ijerph16224429>
- Major Aquifers | Texas Water Development Board. (n.d.). Retrieved July 17, 2022, from <https://www.twdb.texas.gov/groundwater/aquifer/major.asp>
- National Primary Drinking Water Regulations | US EPA. (n.d.). Retrieved August 8, 2023, from <https://www.epa.gov/ground-water-and-drinking-water/national-primary-drinking-water-regulations>
- Pecos Valley Aquifer | Texas Water Development Board. (n.d.). Retrieved July 26, 2022, from <https://www.twdb.texas.gov/groundwater/aquifer/majors/pecos-valley.asp>
- River Basins - Colorado River Basin | Texas Water Development Board. (n.d.). Retrieved July 26, 2022, from [https://www.twdb.texas.gov/surfacewater/rivers/river\\_basins/colorado/index.asp](https://www.twdb.texas.gov/surfacewater/rivers/river_basins/colorado/index.asp)
- Scholarworks@utep, S., & Gardea, M. E. (n.d.). *Water Sourcing Strategies Of Desert Vegetation In Varying Soil Water Sourcing Strategies Of Desert Vegetation In Varying Soil Textures With Vegetation Competition: A Stable Isotope Analysis Textures With Vegetation Competition: A Stable Isotope Analysis*. Retrieved from [https://scholarworks.utep.edu/open\\_etd/3606](https://scholarworks.utep.edu/open_etd/3606)
- Shand, P., Darbyshire, D. P. F., Love, A. J., & Edmunds, W. M. (2009). Sr isotopes in natural waters: Applications to source characterisation and water-rock interaction in contrasting landscapes. *Applied Geochemistry*, 24(4), 574–586. <https://doi.org/10.1016/j.apgeochem.2008.12.011>
- Souchez, R., Lorrain, R., & Tison, J. L. (2002). Les isotopes stables de l'eau et l'environnement physique. *BELGEO*, (2), 133–144. <https://doi.org/10.4000/belgeo.16199>
- Trinity Aquifer | Texas Water Development Board. (n.d.). Retrieved July 31, 2022, from <https://www.twdb.texas.gov/groundwater/aquifer/majors/trinity.asp>
- TSHA | Colorado River. (n.d.). Retrieved July 31, 2022, from <https://www.tshaonline.org/handbook/entries/colorado-river>
- Uliana, M. M., Banner, J. L., & Sharp, J. M. (2007). Regional groundwater flow paths in Trans-Pecos, Texas inferred from oxygen, hydrogen, and strontium isotopes. *Journal of Hydrology*, 334(3–4), 334–346. <https://doi.org/10.1016/j.jhydrol.2006.10.015>
- Vanadium. (n.d.). Retrieved August 8, 2023, from <https://drinktap.org/Water-Info/Whats-in-My-Water/Vanadium>
- Ward, G. H. (n.d.). 3. *Water Resources and Water Supply*. Retrieved from <https://www.researchgate.net/publication/242315971>



Yuan, F., & Miyamoto, S. (2008). Characteristics of oxygen-18 and deuterium composition in waters from the Pecos River in American Southwest. *Chemical Geology*, 255(1–2), 220–230. <https://doi.org/10.1016/j.chemgeo.2008.06.045>

## VITA

Nuria Andreu Garcia earned her Bachelor of Science in Environmental Sciences from The University of Texas at El Paso in August 2019. She researched soil samples from Alaska with Dr. Vanessa Lougheed during her undergraduate studies for three semesters. Following graduation, Nuria joined The Frontera Land Alliance as an Outreach Coordinator.

In Summer 2021, Nuria was admitted to the master's program in Environmental Sciences at The University of Texas at El Paso under the Department of Earth, Environmental, and Resource Sciences (DEERS). She pursued her studies under the guidance of Dr. Lin Ma with a focus on water-stable isotopes. While pursuing her graduate degree, she was part of volunteer work at Frontera and UTEP. Now, she is a full-time hydrologist at HDR Inc. in Sacramento, California.

Contact Information: [nvandreugarcia@gmail.com](mailto:nvandreugarcia@gmail.com)

This thesis was typed by Nuria Andreu